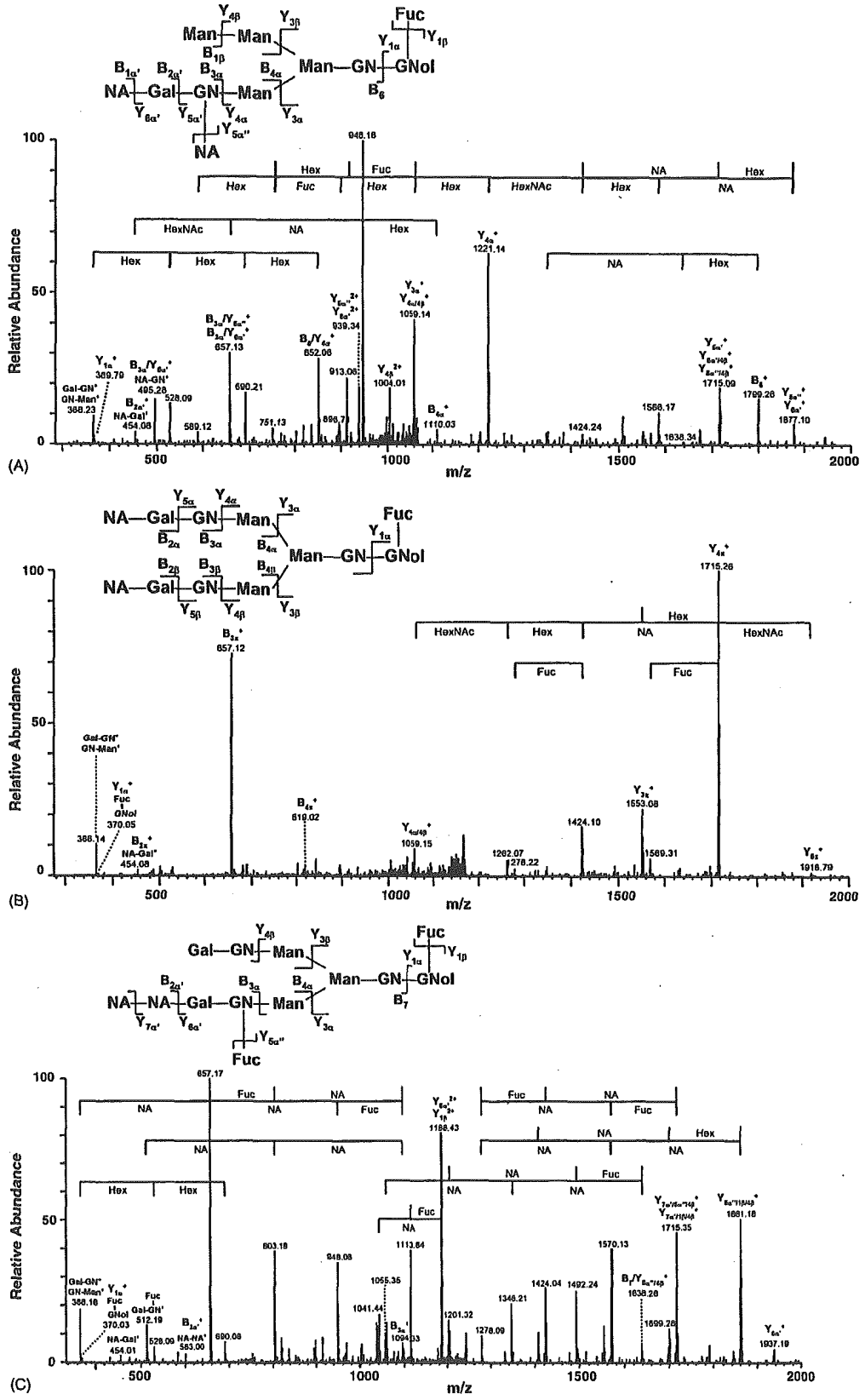

Fig. 7. Product ion spectra of N-linked oligosaccharides of rat brain Thy-1. (A) MS^2 spectrum of $NeuAc_2dHex_1Hex_5HexNAc_2HexNAcol_1$ at *m/z* 1085 (30.4 min). (B) MS^2 spectrum of $NeuAc_2dHex_1Hex_5HexNAc_3HexNAcol_1$ at *m/z* 1187 (42.5 min). (C) MS^2 spectrum of $NeuAc_2dHex_2Hex_5HexNAc_3HexNAcol_1$ at *m/z* 1260 (32.2 min).

In these two studies, we have demonstrated a strategy for glycosylation analysis of Thy-1, including identification of a glycoprotein, determination of glycosylation sites, site-specific glycosylation analysis, and structural analysis of oligosaccharide details. This strategy can be applied to glycosylation analysis of other glycoproteins. Specifically, the glycoprotein sample is divided into two. One is subjected to proteinase digestion followed by peptide/glycopeptide mapping, which provides information on glycosylation sites and site-specific heterogeneity. The other is subjected to PNGase F digestion followed by mass spectrometric oligosaccharide profiling, by which a detailed structure of *N*-glycans released from a glycoprotein could be provided. Recently, proteomic approaches, which are based on two-dimensional electrophoresis followed by mass spectrometry, have been used in various fields. Although glycosylation analysis of abundant glycoproteins in gel has been successful, that of a low-abundance glycoprotein in gel remains a great challenge. The proposed method consisting of peptide/glycopeptide mapping followed by oligosaccharide profiling with sequential scans by IT–MS-FT–ICR–MS will likely be a powerful tool for glycosylation analysis of low-abundance glycoproteins and for proteomics/glycomics.

Acknowledgements

This work was supported in part by a Grant-in-Aid for Creative Scientific Research (16GS0313) from the Ministry of Education, Culture, Sports, and Technology, the Ministry of Health, Labor and Welfare, and Core Research for the Evolutional Science and Technology Program (CREST) of the Japan Science and Technology Agency (JST).

We appreciate Dr. A. Hachisuka of the National Institute of Health Science for her technical advice.

We thank Dr. M. Kubota and Mr. M. Yoshida of Thermo Electron K.K. (Japan) for their technical support.

References

[1] A. Varki, Glycobiology 3 (1993) 97.
[2] J.W. Dennis, M. Granovsky, C.E. Warren, Biochim. Biophys. Acta 1473 (1999) 21.
[3] Y. Sato, M. Kimura, C. Yasuda, Y. Nakano, M. Tomita, A. Kobata, T. Endo, Glycobiology 9 (1999) 655.
[4] G. Durand, N. Seta, Clin. Chem. 46 (2000) 795.
[5] O. Krokhin, W. Ens, K.G. Standing, J. Wilkins, H. Perreault, Rapid Commun. Mass Spectrom. 18 (2004) 2020.
[6] Y. Satomi, Y. Shimonishi, T. Takao, FEBS Lett. 576 (2004) 51.
[7] Y. Wada, M. Tajiri, S. Yoshida, Anal. Chem. 76 (2004) 6560.
[8] W. Chai, V. Piskarev, A.M. Lawson, Anal. Chem. 73 (2001) 651.
[9] D. Sagi, J. Peter-Katalinic, H.S. Conradt, M. Nimtz, J. Am. Soc. Mass Spectrom. 13 (2002) 1138.
[10] A. Zamfir, D.G. Seidler, H. Kresse, J. Peter-Katalinic, Glycobiology 13 (2003) 733.
[11] D.J. Harvey, R.L. Martin, K.A. Jackson, C.W. Sutton, Rapid Commun. Mass Spectrom. 18 (2004) 2997.
[12] C. Robbe, C. Capon, B. Coddeville, J.C. Michalski, Rapid Commun. Mass Spectrom. 18 (2004) 412.
[13] N. Ojima, K. Masuda, K. Tanaka, O. Nishimura, J. Mass Spectrom. 40 (2005) 380.
[14] C.W. Sutton, J.A. O'Neill, J.S. Cottrell, Anal. Biochem. 218 (1994) 34.
[15] B. Küster, S.F. Wheeler, A.P. Hunter, R.A. Dwek, D.J. Harvey, Anal. Biochem. 250 (1997) 82.
[16] B. Küster, T.N. Krogh, E. Mortz, D.J. Harvey, Proteomics 1 (2001) 350.
[17] K. Hirayama, R. Yuji, N. Yamada, K. Kato, Y. Arata, I. Shimada, Anal. Chem. 70 (1998) 2718.
[18] F. Wang, A. Nakouzi, R.H. Angeletti, A. Casadevall, Anal. Biochem. 314 (2003) 266.
[19] K. Sandra, I. Stals, P. Sandra, M. Claeyssens, J. Van Beeumen, B. Devreese, J. Chromatogr. A 1058 (2004) 263.
[20] Y. Satomi, Y. Shimonishi, T. Hase, T. Takao, Rapid Commun. Mass Spectrom. 18 (2004) 2983.
[21] A. Harazono, N. Kawasaki, T. Kawanishi, T. Hayakawa, Glycobiology 15 (2005) 447.
[22] M. Wuhrer, C.A. Koeleman, C.H. Hokke, A.M. Deelder, Anal. Chem. 77 (2005) 886.
[23] B.L. Schulz, N.H. Packer, N.G. Karlsson, Anal. Chem. 74 (2002) 6088.
[24] N.L. Wilson, B.L. Schulz, N.G. Karlsson, N.H. Packer, J. Proteome Res. 1 (2002) 521.
[25] L.A. Gennaro, D.J. Harvey, P. Vouros, Rapid Commun. Mass Spectrom. 17 (2003) 1528.
[26] N.G. Karlsson, B.L. Schulz, N.H. Packer, J. Am. Soc. Mass Spectrom. 15 (2004) 659.
[27] N.G. Karlsson, N.L. Wilson, H.J. Wirth, P. Dawes, H. Joshi, N.H. Packer, Rapid Commun. Mass Spectrom. 18 (2004) 2282.
[28] M. Wuhrer, C.A. Koeleman, A.M. Deelder, C.H. Hokke, Anal. Chem. 76 (2004) 833.
[29] Y. Takegawa, K. Deguchi, S. Ito, S. Yoshioka, H. Nakagawa, S. Nishimura, Anal. Chem. 77 (2005) 2097.
[30] S. Itoh, N. Kawasaki, M. Ohta, T. Hayakawa, J. Chromatogr. A 978 (2002) 141.
[31] S. Itoh, N. Kawasaki, A. Harazono, N. Hashii, Y. Matsuishi, T. Kawanishi, T. Hayakawa, J. Chromatogr. A 1094 (2005) 105.
[32] N. Kawasaki, M. Ohta, S. Hyuga, O. Hashimoto, T. Hayakawa, Anal. Biochem. 269 (1999) 297.
[33] S. Itoh, N. Kawasaki, M. Ohta, M. Hyuga, S. Hyuga, T. Hayakawa, J. Chromatogr. A 968 (2002) 89.
[34] N. Kawasaki, S. Itoh, M. Ohta, T. Hayakawa, Anal. Biochem. 316 (2003) 15.
[35] C. Bordier, J. Biol. Chem. 256 (1981) 1604.
[36] M.P. Lisanti, M. Sargiacomo, L. Graeve, A.R. Saltiel, E. Rodriguez-Boulan, Proc. Natl. Acad. Sci. U.S.A. 85 (1988) 9557.
[37] B. Domon, C.E. Costello, Glycoconjugate J. 5 (1988) 397.
[38] C. Sato, T. Matsuda, K. Kitajima, J. Biol. Chem. 277 (2002) 45299.

MINIREVIEW

Trends in Glycoscience and Glycotechnology
Vol.17 No.97 (September 2005) pp.193–203

Mass Spectrometry of Glycoproteins

糖タンパク質の質量分析

Kawasaki, Nana*[1,2]; Itoh, Satsuki[1]; Harazono, Akira[1]; Hashii, Noritaka[1,2]; Matsuishi, Yukari[1,2]
Hayakawa, Takao[3]; and Kawanishi, Toru[1]

[1]Division of Biological Chemistry and Biologicals, National Institute of Health Science,
1-18-1, Kamiyoga, Setagaya-ku, Tokyo, 158-8501, Japan

[2] Core Research for Evolutional Science and Technology (CREST) of Japan Science and Technology Agency (JST),
Kawaguchi Center Building, 4-1-8, Hon-cho, Kawaguchi, Saitama 332-0012, Japan

[3] Pharmaceutical and Medical Devices Agency, 3-3-2 Kasumigaseki, Chiyoda-ku, Tokyo, 100-0013, Japan

*Correspondence to: Nana Kawasaki, National Institute of Health Sciences,
Division of Biological Chemistry and Biologicals, 1-18-1 Kamiyoga, Setagaya-ku, Tokyo, 158-8501, Japan
FAX: 81-3-3700-9084, E-mail: nana@nihs.go.jp

Key Words: *MS, MS/MS, MS^n, glycoprotein, oligosaccharide, glycopeptide*

Abstract

This review presents mass spectrometric methods for glycoprotein identification; determination of glycosylation sites, structural elucidation of carbohydrates, and their applications to glycomics and proteomics.

要　約

本レビューでは、質量分析を用いた糖タンパク質同定、糖鎖結合位置の決定、糖鎖構造解析、及びグライコミクス・プロテオミクスへの応用について紹介する。

A. Introduction

Mass spectrometry (MS) has become a powerful tool for glycoprotein identification, and the determination of glycosylation sites, and structural features of carbohydrates, such as sequence, linkage and branching at each glycosylation site. Generally, the mass spectrometric characterization of glycoprotein involves the following steps: 1) fractionation of enzymatically or chemically liberated glycans followed by MS, and 2) fractionation of glycopeptides from proteolytic digests followed by MS. Here we present the MS of glycan and glycopeptides using the latest applications.

B. MS of Liberated Glycans

Matrix-assisted laser desorption/ ionization (MALDI) (1), and electrospray ionization (ESI) (2), which are soft ionization techniques, are often used for glycan molecular mass determination. MALDI has been used by preference for rapid microanalyses, however, it generates metastable ions and the consequent various fragmentations, including the depletion of terminal sialic acids (known as post-source decay, PSD) (3). Although ESI used to have a problem with sensitivity, the introduction of nanospray technology allows us to use ESI to analyze femtomole levels of glycans (4). To measure all types of glycans, including neutral glycans and sulfated or sialylated acidic glycans, we suggest mass spectrometric glycan analysis in both positive and negative ion modes.

MALDI and ESI are combined with several types of

A. 緒　言

質量分析 (MS) は、糖タンパク質の同定、糖鎖結合位置の決定、並びに各結合位置における糖鎖の配列、結合位置、及び分岐等を含む構造特性解析の有用な手段として利用されている。現在、MS を用いた糖鎖解析のアプローチとしては、1) 酵素的または化学的に切り出された糖鎖の分画と MS、及び 2) 糖タンパク質酵素消化物からの糖ペプチドの分画と MS、が一般的である。そこで、ここでは、遊離糖鎖と糖ペプチドの MS について、最近の分析例を取り上げながら解説する。

B. 遊離糖鎖の MS

糖鎖分子の分析に適したソフトイオン化法として、マトリクス支援レーザー脱離イオン化法 (MALDI) (1)、及びエレクトロスプレーイオン化法 (ESI) (2) がよく利用されている. MALDI は迅速分析及び微量分析に適しているが、準安定イオンが生成し、MS^1 スペクトル上にはシアル酸が脱離したイオンをはじめとする様々なフラグメントが検出される (ポストソース分解、PSD) (3)。ESI は感度上の問題が指摘されてきたが、現在ではナノスプレーの開発によって、フェムトモルレベルの糖鎖分析が可能となっている (4)。糖鎖には中性糖鎖だけでなく、シアル酸や硫酸基などが結合した酸性糖鎖が存在するので、未知試料を分析する際には、ポジティブ及びネガティブ両イオンモードで測定するのが望ましい。

MALDI や ESI は様々なアナライザー (分析計) と組み合

analyzer, such as quadrupole (Q) (5), quadrupole ion trap (IT) (6), time-of-flight (TOF) (7), and Fourier transform ion cyclotron resonance (FTICR) (8). Tandem mass spectrometers with various combinations of these analyzers have recently become available. Tandem mass spectrometry (MS/MS) is widely recognized as an effective means of structural elucidation, including molecular mass measurement by MS^1 and oligosaccharide sequencing by collision-induced dissociation (CID)-MS/MS (9–11). In particular, ITMS instruments are becoming popular for multistage tandem mass spectrometry (MS^n), which offers multiple precursor selections and CID experiments (12, 13).

Fig. 1A shows types of carbohydrate fragmentation by CID-MS/MS (14). In the positive ion mode the most common fragmentation involves cleavage of the glycosidic bond with retention of the glycosidic oxygen atom by species formed from the reducing end (Fig. 1B). Fragment ions generated by this cleavage are represented as B-ion (non-reducing end) and Y-ion (reducing end). The cleavage of carbon-carbon bonds of the sugar ring yields A-ion and X-ion. These cross ring fragments are often used as decisive ions in linkage determination (15, 16).

Fig. 2 shows the positive ion ESI-MS/MS and MS^3 spectra of pyridylaminated agalacto-triantennary oligosaccharide (I) (Figs. 2A, A') and bisected agalacto-biantennary oligosaccharide (II) (Figs. 2B, B'). These are positional isomers whose one GlcNAc is attached to either α1-3/6 Man or β1-4Man in the trimannosyl core and cannot

わせて利用されている。アナライザーには四重極型 (Q) (5)、イオントラップ型 (IT) (6)、飛行時間型 (TOF) (7)、及びフーリエ変換イオンサイクロトロン共鳴型 (FTICR) (8) MS 装置などが用いられている．現在では、これらの分析装置を様々に組み合わせたタンデム質量分析装置の利用が可能である。タンデム質量分析 (MS/MS) は、MS^1 による糖鎖の質量測定と、衝突誘起解離 (CID)-MS/MS による糖鎖の配列解析を同時に行うことができる (9–11)。特に ITMS 装置は、前駆イオンの選択と CID-MS/MS を繰り返す多段階 MS/MS (MS^n) が可能であることから、近年、糖鎖解析用装置としての人気が高い (12、13)。

図 1A は、CID-MS/MS における糖鎖の開裂を示したものである (14)。ポジティブイオンモードで測定した糖鎖の CID-MS/MS では主に、グリコシド結合の酸素原子を還元末端側糖鎖に残した開裂が生じる (図 1B)．そのとき生じた非還元末端側イオンは B イオン、還元末端側イオンは Y イオンと呼ばれ、糖鎖の配列解析に利用される。ピラノース環の炭素 - 炭素間の結合が開裂して生じたイオンは A、及び X イオンと呼ばれ、糖鎖結合位置の決め手となることがある (15、16)。

図 2 は、ピリジルアミノ化されたアガラクト 3 本鎖糖鎖 (I) 及びアガラクトバイセクト 2 本鎖糖鎖 (II) のポジティブイオン MS/MS (図 2A、B)、及び MS^3 (図 2A'、B') スペクトルである。これらの糖鎖は GlcNAc 1 分子がトリマンノシルコアの α1-3/6Man または β1-4Man に結合した位置異性体で、MS^1 による分子量測定では区別することはできない。しかし、MS^n によっ

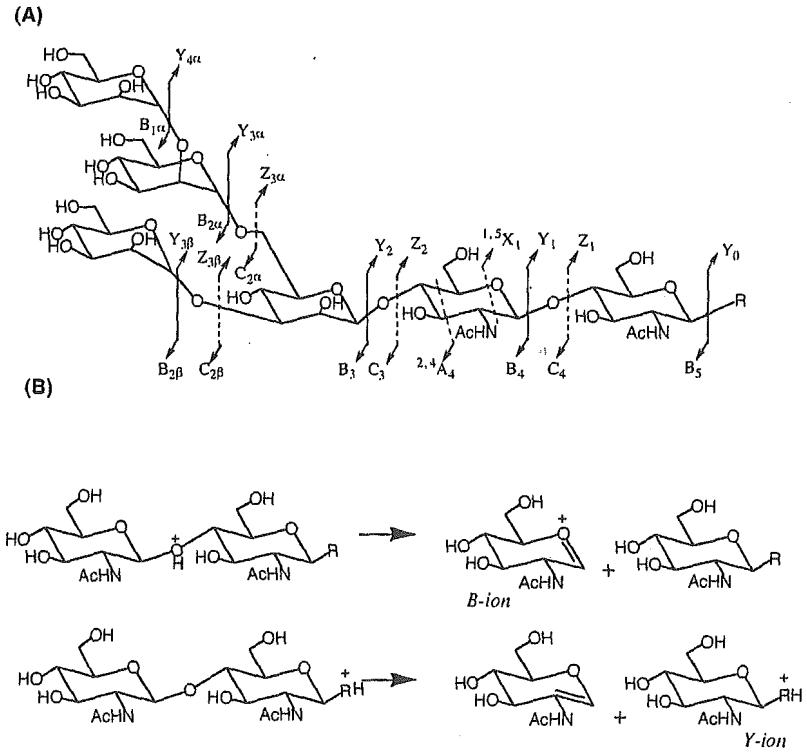

Fig. 1. (A) Types of carbohydrate fragmentation. (B) Production of B- and Y-ions in the positive ion mode.

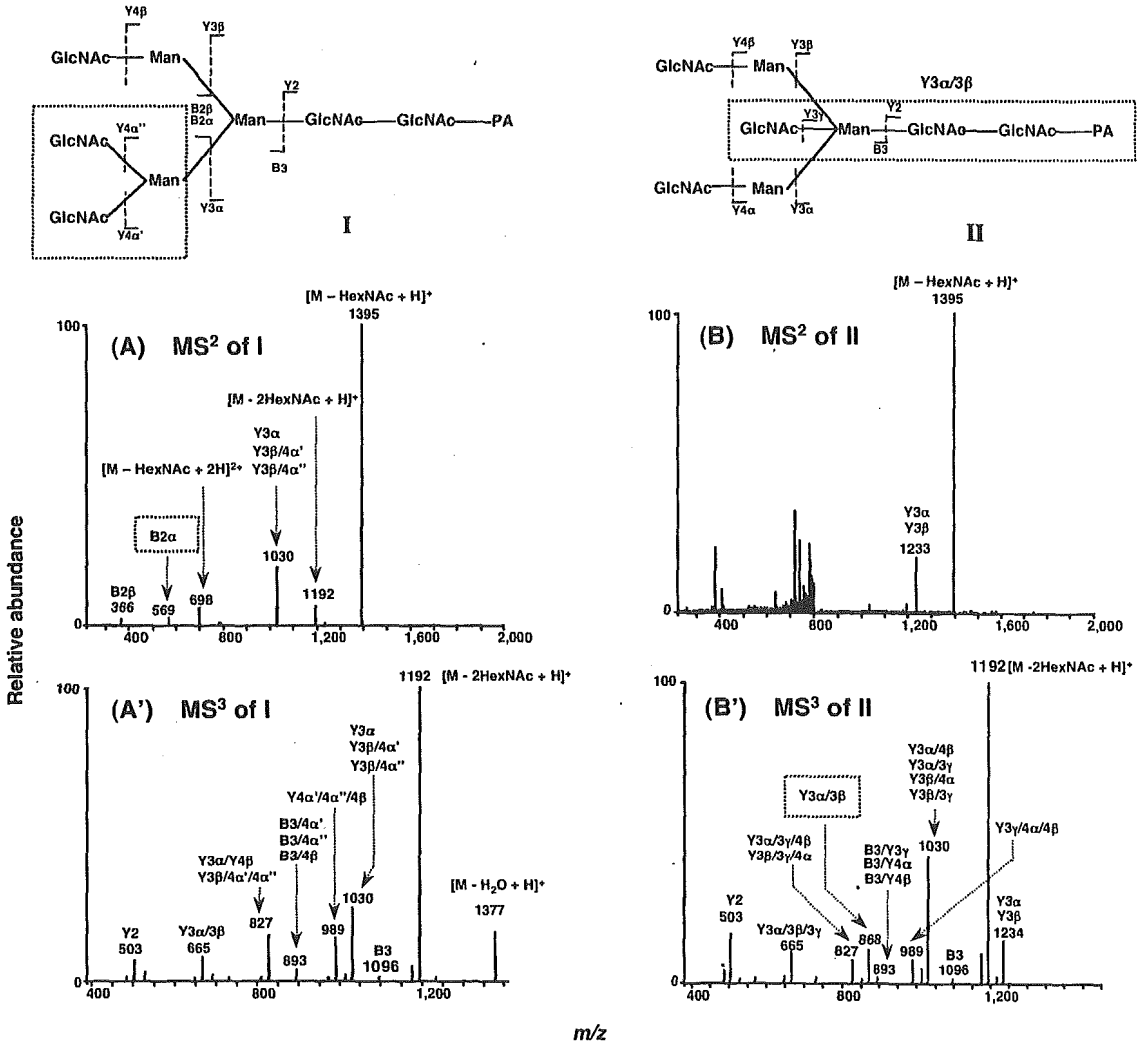

Fig. 2. MS^n spectra of oligosaccharides. (A) MS/MS spectrum of oligosaccharide I (precursor ion: *m/z* 800.8). (A') MS^3 spectrum of oligosaccharide I (precursor ion: *m/z* 1,395.4). (B) MS/MS spectrum of oligosaccharide II (precursor ion: *m/z* 800.5). (B') MS^3 spectrum of oligosaccharide II (precursor ion: *m/z* 1,395.4). MS: LTQ (Thermo Electron).

be discriminated by MS^1 (molecular mass determination). In contrast, MS^n spectra clearly show structural differences between two glycans. B-ion corresponding to $GlcNAc_2Man^+$ is observed at *m/z* 569 in the MS/MS spectrum of glycan I (Fig. 2A), while Y-ion at *m/z* 868 corresponding to [GlcNAc-Man-GlcNAc-GlcNAc-PA + H]$^+$ is detected in MS^3 spectrum of glycan II (Fig. 2B'). In particular, glycan II can be determined as bisected oligosaccharides on the basis of a bisected *N*-glycan diagnostic ion at *m/z* 868.

The MS^n spectra of some glycans exhibit characteristic fragment patterns. Hence, even if no diagnostic ion, such as a bisected glycan-specific fragment, is detected, the glycan structure can be sometimes deduced from ion intensity ratios obtained by MS^n (17,18). For instance, structures of branched arms were deduced from mass spectrometric patterns obtained by MS/MS which causes a cleavage of α1-3 linkage more than α1-6 linkage (19–21). However, complete structural

糖鎖 I の MS/MS スペクトルには *m/z* 569 に $GlcNAc_2Man^+$ に相当する B イオンが検出され（図 2A）、糖鎖 II の MS^3 スペクトル（前駆イオン：*m/z* 1395 [M-HexNAc + H]$^+$）には [GlcNAc-Man-GlcNAc-GlcNAc-PA + H]$^+$ に 相当するイオンが *m/z* 868 に検出されている（図 2B'）。特に、[GlcNAc-Man-GlcNAc-GlcNAc-PA + H]$^+$ (*m/z* 868) はバイセクト糖鎖に特異的なフラグメントであり、糖鎖 II がバイセクト糖鎖であることを決定づけている。

糖鎖の MS^n は特徴的なスペクトルパターンを示すことが多いので、構造特異的イオンが検出されない場合でも、MS^n スペクトルのパターンより糖鎖構造を推定できる場合がある (17,18)。例えば、トリマンノシルコアの α1-3 結合が α1-6 結合よりも開裂しやすいことを利用して、分岐構造を解析した例が報告されている (19–21)。しかし、MS 単独で糖鎖構造を完

elucidation by MS alone is still a great challenge, and additional experiments are required, such as exoglycosidase digestion (22), lectin affinity chromatography (23), and sugar mapping (17,24,25).

C. Glycan Profiling by LC/MS

Many different oligosaccharides are attached to a glycoprotein. The development of derivatization and separation techniques for glycans has been an important part of structural glycobiology (26–34). The derivatization of glycan with a hydrophobic molecule improves the ionization efficiency of hydrophilic glycans and offers higher sensitivity (31,35). A combination of various HPLC techniques with off-line MALDI-MS or on-line ESI-MS has been successful in oligosaccharide profiling as well as the elucidation of structural details (36–39). As an example, we present the mass spectrometric *N*-glycan profiling of CHO cells and cells transfected with *N*-acetylglucosaminyltransferase III, which catalyzes the addition of GlcNAc to β1-4Man in the trimannosyl core (Fig. 3) (40). Mass spectrometric analysis reveals the difference in glycosylation between two samples and the appearance of peaks with additional HexNAc (203 Da) in the transfected cells.

We recently demonstrated quantitative oligosaccharide

全に同定することが困難である場合が多く、MS はエキソグリコシダーゼによる段階的消化法 (22)、レクチンアフィニティークロマトグラフィー (23)、及び糖鎖マッピング (17、24、25) などと組み合わせて用いられることが多い。

C. LC/MS を用いた糖鎖プロファイリング

糖タンパク質には様々な糖鎖が結合しているので、糖鎖の標識法と分離技術の開発は、構造糖鎖生物学において重要な位置を占めている (26–34)。糖鎖を分離・検出するために開発された疎水性物質による誘導体化は、親水性の高い糖鎖のイオン化効率を向上させるので、MS における高感度化においても有用である (31、35)。さらに、様々な HPLC による分離法とオフライン MALDI-MS、あるいはオンライン ESI-MS を組み合わせた分析方法は、糖鎖プロファイリングと糖鎖構造解析を兼ね備えた方法として利用され、多くの成果を上げている (36–39)。一例として図 3 に CHO 細胞、及びトリマンノシルコアの β1-4Man に GlcNAc を付加させる *N*- アセチルグルコサミン転移酵素 III (GnT-III) 遺伝子を導入した CHO 細胞の MS を用いた糖鎖プロファイリングの結果を示す (40)。MS を利用することによって、GnT-III 導入細胞で新たに出現した糖鎖は、HexNAc1 分子 (203Da) 増加した糖鎖であることが確認できる。

筆者らは最近、安定同位体標識化 2- アミノピリジン (AP) を用いた標識法と LC/MS を組み合わせた定量的糖鎖プロファ

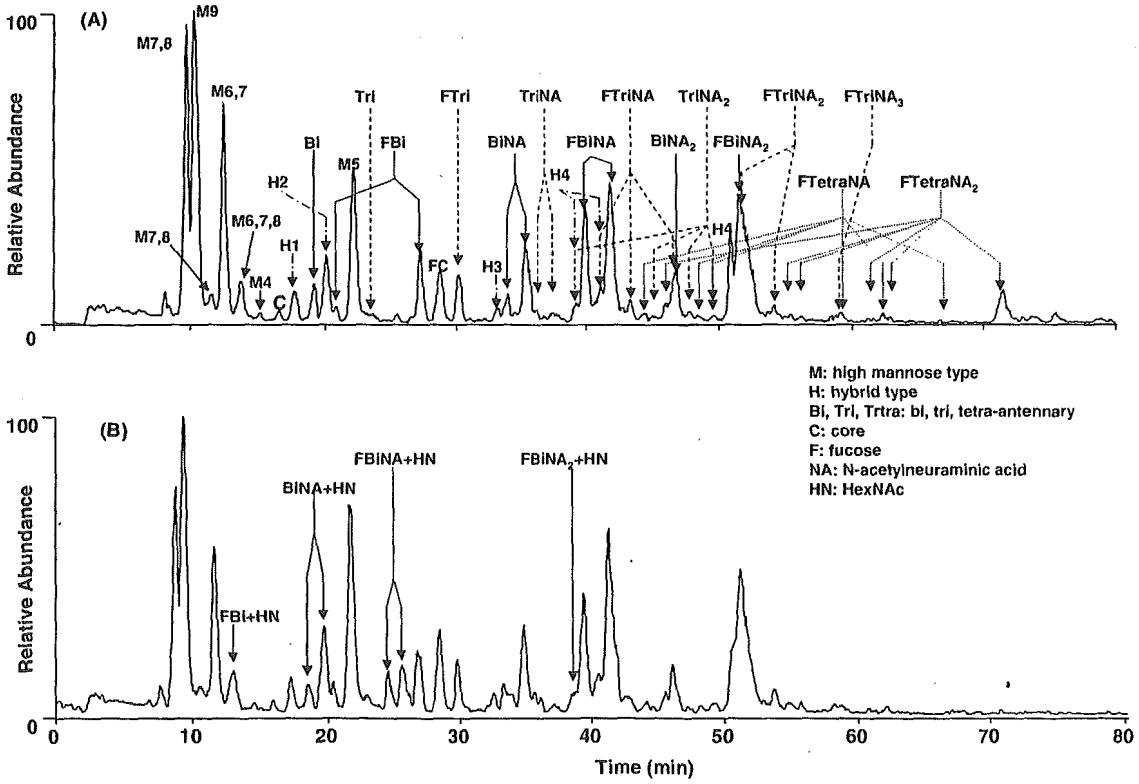

Fig. 3. TICs of *N*-linked oligosaccharides released from the insoluble fractions. (A) CHO cells. (B) *N*-acetyl glucosaminyltransferase III-transfected CHO cells. Column: Hypercarb (0.2 × 150 mm, Thermo Electron), LC: Magic 2002 (Michrome BioResources), MS: TSQ-7000 (Thermo Electron), Eluent: 5 mM ammonium acetate containing acetonitrile.

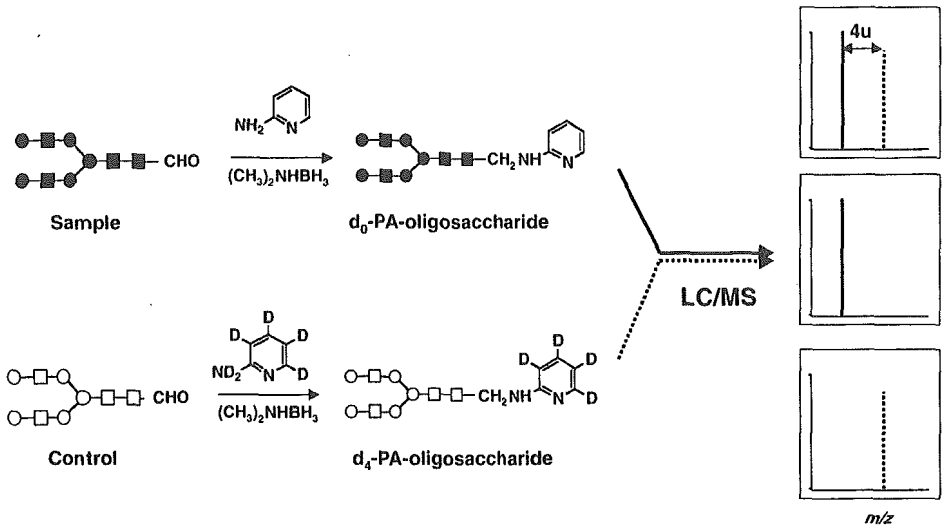

Fig. 4. Quantitative oligosaccharide profiling using LC/MS and an isotope tagging method.

profiling using isotope-labeled 2-aminopyridine (AP) and LC/MS (Fig. 4) (41). In this procedure, oligosaccharides released from an analyte and standard glycoprotein are tagged with d_0-AP and d_6-AP, respectively, and an equal amount of d_0-PA and d_4-PA oligosaccharides is analyzed by LC/MS. Oligosaccharides existing in either the analyte or standard glycoprotein appear as single ions, and oligosaccharides that exist in both analyte and standard glycoprotein are detected as paired ions with a difference of 4 u. The relative amount of analyte oligosaccharides can be determined on the basis of the analyte/ internal standard ion pair intensity ratio. This method can improve the precision of the mass spectrometric quantification and be used for glycan differential analysis among multiple samples.

D. MS of Glycopeptides

When glycans are released from protein, all information about their attachment to the protein is lost. Protein identification, determination of glycosylation sites and site-specific glycosylation analyses are generally achieved by the mass spectrometric analysis of glycopeptides. ESI and MALDI coupled with several analyzers are employed for glycopeptide analysis. ESI allows the accurate mass measurement of relatively large glycopeptide/protein because of the generation of multiple charged ions, whereas ions of large glycopeptide molecule ions are sometimes missed by MALDI-MS due to PSD and their poor ionization efficiency (42).

Fig. 5 illustrates three possible cleavages of the peptide backbone. The most common C-terminal and N-terminal fragment ions are b-ion and y-ion, respectively (37). In many cases, CID induces glycosidic bond cleavages rather than peptide backbones. Electron capture dissociation with FT-ICRMS is reported as a means for preferential cleavage of the

イリングを開発した(図4)(41)。この方法は、標準糖タンパク質及び検体糖タンパク質から切り出した糖鎖をそれぞれ6重水素置換AP(d_6-AP)、及び未置換AP (d_0-AP)で標識し、得られたd_4-PA糖鎖及びd_0-PA糖鎖を1対1の混合物としてLC/MSで分析するものである。標準糖タンパク質または検体糖タンパク質のどちらか一方にしか結合していない糖鎖は、d_4-PA糖鎖またはd_0-PA糖鎖どちらかの単独イオンとして検出される。標準糖タンパク質及び検体糖タンパク質に共通して存在する糖鎖は4u異なる1対のイオンとして検出され、d_4-PA糖鎖及びd_0-PA糖鎖のイオン強度比から相対糖鎖結合量を求めることができる。同位体標識糖鎖を内部標準物質として用いることによって、MSを用いた定量解析における再現性が改良されるので、定量的糖鎖プロファイリングは、複数のサンプル間の糖鎖の差異を質的量的に比較する場合に有用である。

D. 糖ペプチドのMS

タンパク質から糖鎖を切り離すと、糖鎖とタンパク質間の結合に関する情報が失われてしまうので、糖鎖含有タンパク質の同定、糖鎖結合位置の決定、及び部位特異的糖鎖不均一性の解析などには糖ペプチドのMSが適している。糖ペプチドの分析においても、ESIあるいはMALDIに様々なアナライザーを組み合わせた装置が利用されている。MALDI-MSでは、ほぼ一価イオンが生成するが、ESI-MSでは多価イオンが生成するため比較的高分子量の糖ペプチドの質量を正確に測定することが可能である。また、MALDI-MSを用いて糖鎖の割合が高い糖ペプチドを分析する場合、イオン化の抑制やPSDによって、分子関連イオンが測定されにくいとする報告がある(42)。

図5はペプチド骨格の開裂を示している。ペプチド結合の開裂によって生じたN末端側はbイオン、C末端側はyイオンと呼ばれる(43)。通常、糖ペプチドのCID-MS/MSでは、ペプチドよりも糖鎖の開裂が優先される。ペプチド部分が優先的に開裂する方法としてFT-ICRMS装置を用いた電子捕獲解

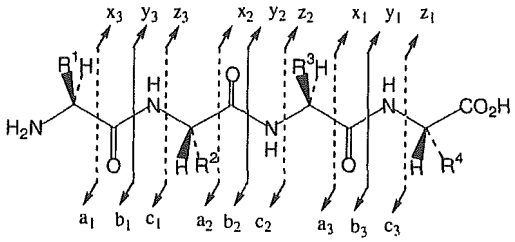

Fig. 5. Types of peptide fragmentation.

peptide backbone (44,45).

For the cleavages of both glycosidic and peptide bonds CID-MS/MS is carried out with relatively high energy (approx. 50V/1000 u) (46–51). Hence, it allows both peptide sequencing and estimation of the carbohydrate structure on the basis of b/y-ions and B/Y-ions. Fig. 6A presents the CID-MS/MS spectrum of a glycopeptide derived from human α-fetoprotein using the ESI-QqTOFMS instrument. Carbohydrate-specific B-ions, such as $HexNAc^+$ and $NeuAc^+$ are observed at *m/z* 204, 292 as well as y-series ions. Based on the y-series ions and peptide ion, this peptide is identified

糖鎖とペプチド部分を同時に開裂させるためには比較的高いエネルギー(約50V/1000 u)を与えてCID-MS/MSを行う(46–51)。生成したb、yイオン、及びB、Yイオンから、ペプチド部分のアミノ酸配列や、糖鎖構造を解析することができる。図6Aは、ESI-四重極飛行時間型MSを用いたCID-MS/MSによって得られたヒトアルファフェトプロテイン由来糖ペプチドのMS/MSスペクトルである。糖鎖Bイオンである*m/z* 204 ($HexNAc^+$)、及び292 ($NeuAc^+$)等と一緒に、ペプチドに由来する一連のyイオンが検出されていることがわかる。これら一

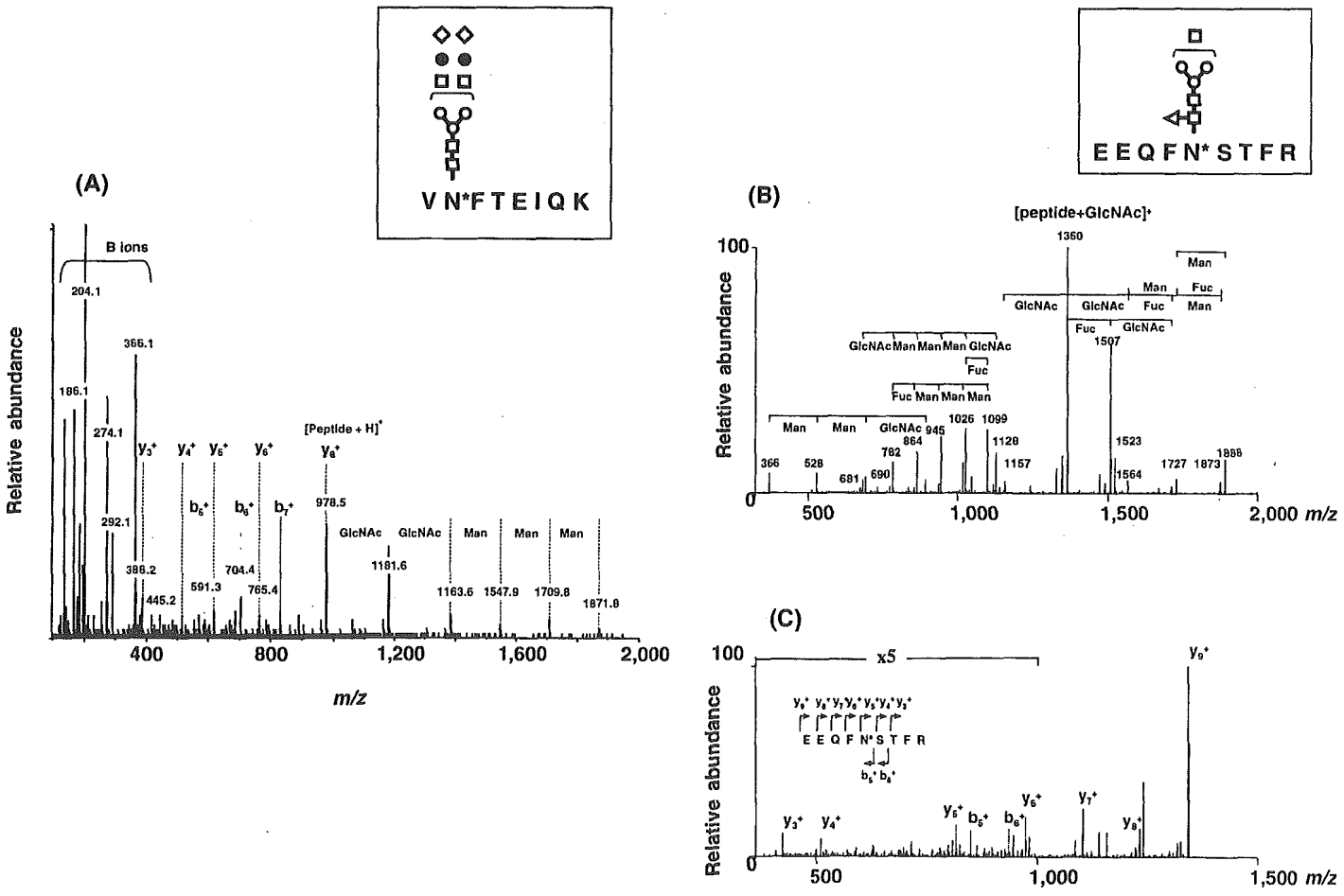

Fig. 6. CID-MS^n spectra of glycopeptides. (A) CID-MS/MS with relatively high energy (precursor ion, *m/z* 1,061.8), Sample: glycopeptide from human alpha-fetoprotein, MS: QSTAR (Applied Biosystems). (B) Low-energy CID-MS/MS (precursor ion, *m/z* 1,200). (C) Low-energy CID-MS^3 (precursor ion, *m/z* 1,360), Sample: glycopeptide from mouse IgG1, MS: LTQ (Thermo Electron).

as VNFTEIQK. The oligosaccharide structure can be deduced as disialylated biantennary from the molecular mass of the carbohydrate moiety together with B-ions in the MS/MS spectrum.

B- and Y-series ions are produced by the low-energy CID-MS/MS of glycopeptides (12, 52–55). Fig. 6B shows the low energy (approx. 5–20V/1000 u) CID-MS/MS spectrum of glycopeptide derived from mouse IgG1. Based on the carbohydrate related-ions, the carbohydrate structure could be determined as fucosylated biantennary. When using an ITMS instrument, MS^3 is automatically carried out for intense ions. In this experiment, [peptide +HexNAc +H]$^+$, which is generally detected as intense ion, was subjected to further product ion scan, and b- and y-series ions appeared in the MS^3 spectrum (Fig. 6C). Peptides can be identified by comparing experimental fragment ions with predictable fragment ions derived from proteins in a database. Moreover, the database analysis with the possibility of glycosylation at Asn and Ser/Thr with HexNAc, Hex, and dHex allows the identification of glycopeptides and glycosylation sites (56). For instance, this peptide was identified as EEQFN*STFR glycosylated with HexNAc at N*. This method would enable the glycosylation analysis of unknown glycoproteins and a mixture of glycoproteins.

E. Site-Specific Glycosylation Analysis of Glycoproteins

Fig. 7 illustrates the strategy for the site-specific glycosylation analysis of glycoproteins. First, a glycoprotein is digested with an appropriate proteinase, which provides

連のｙイオン、及びペプチドイオンの質量から、このペプチド部分はVNFTEIQKと同定することができる。また、糖鎖構造は、糖鎖部分の分子量とＢイオンからジシアロ２本鎖糖鎖と推定される。

低エネルギーCID-MS/MSでは、グリコシド結合が優先して開裂し、B、及びＹイオンが検出される(12、52–55)。図6Bはマウス IgG1 から得られた糖ペプチドの低エネルギーCID-MS/MS (約5-20V/1000 u) スペクトルで、糖鎖関連イオンから、糖鎖構造を推定することができる。糖ペプチドのMS/MSでは一般に、[ペプチド + HexNAc + H]$^+$が比較的強く検出される。そこで、ITMS装置を用いて[ペプチド +HexNAc + H]$^+$を前駆イオンとして選択し、さらにプロダクトイオンスキャンを行うと、MS^3スペクトル上にｂ及びｙイオンが検出される(図6C)。これらのｂ及びｙイオンの実測値をタンパク質データベースに登録されているタンパク質の予測プロダクトイオンの理論質量と比較することによって、ペプチドを同定することができる．さらに、AsnやSer/ThrにHexNAc、Hex、あるいはdHex等による糖鎖修飾の可能性を追加してデータベース検索をすることによって、糖鎖結合位置を決定できる場合がある(56)。例えば、ここで分析された糖ペプチドはデータベース検索エンジンを用いて、EEQFN*STFR(N*はHexNAc修飾Asn)と同定された。この方法を利用することによって、混合物中の糖タンパク質や、未知の糖タンパク質の部位特異的な糖鎖解析が可能となるものと期待される。

E. 糖タンパク質の部位特異的糖鎖解析

糖タンパク質の部位特異的糖鎖解析の流れを図7にまと

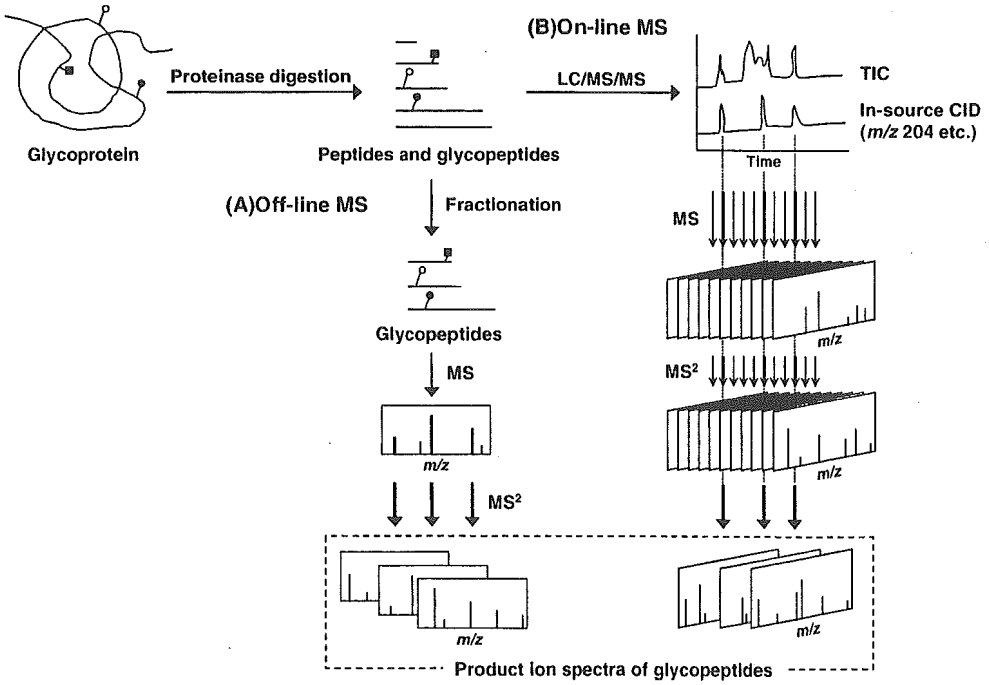

Fig. 7. Strategy for site-specific glycosylation analysis by LC off-line MS (A) and on-line LC/MS (B).

glycopeptides, including a single glycosylation site. Trypsin, Lys-C, Glu-C and Asp-N are commonly used for glycosylation analysis. Since glycopeptide ions are sometimes missed by MS in the presence of excess peptides due to their lower ionization efficiency, several methods have been proposed for the fractionation of glycopeptides, such as HPLC and affinity chromatography (57,58), followed by off-line MALDI-MS. LC on-line ESI/MS is an efficient method for the direct elucidation of glycopeptides in a complex mixture. Although LC/MS provide a complicated chromatogram, glycopeptides in a choromatographic position can be localized by the appearance of marker ions, such as $HexNAc^+$ and $HexHexNAc^+$, resulting from precursor ion scanning and in-source CID (59–66). However, for peptide identification these two means require additional CID-MS/MS scan for some intense ions (data-dependent CID-MS/MS scan). Recently we presented an alternative method, with which product ion spectra of glycopeptides can be selected directly using marker ions arising from glycopeptides by data-dependent CID-MS/MS scan with relatively high energy (49).

める。まず、糖タンパク質を適切な酵素で糖ペプチドに断片化する。この際、同一ペプチドに複数の糖鎖結合部位が含まれないように酵素を選択する。基質特異性の高いトリプシン、Lys-C、Glu-C、及びAsp-N等がよく用いられている。糖ペプチドはペプチドに比べてイオン化効率が悪く、ペプチドが混在するとマススペクトルが得られにくい。そのため、アフィニティークロマトグラフィーや、HPLC等で予め糖ペプチドを分画してから(57,58)、マススペクトルを測定するオフライン法(図7A)や、C18カラム等を用いたLC/MSでペプチド・糖ペプチドを分離しながら直接マススペクトルを測定するオンライン法がよく用いられている(図7B)。オンラインLC/MSでは複雑なクロマトグラムが得られるが、プリカーサーイオンスキャンやインソースCIDによって生じた糖鎖に特徴的なBイオン(例えば、$HexNAc^+$、*m/z* 204や$HexHexNAc^+$、*m/z* 366など)を利用することによって、糖ペプチドの溶出位置を推定することができる(59–66)。ただしこれらの方法は、ペプチドを同定するために、別途、強度の高いイオンに対する自動的CID-MS/MSスキャン(データ依存的CID-MS/MSスキャン)を行う必要がある。そこで、我々は別法として、データ依存的なCID-MS/MSによって生成したBイオンを利用して糖ペ

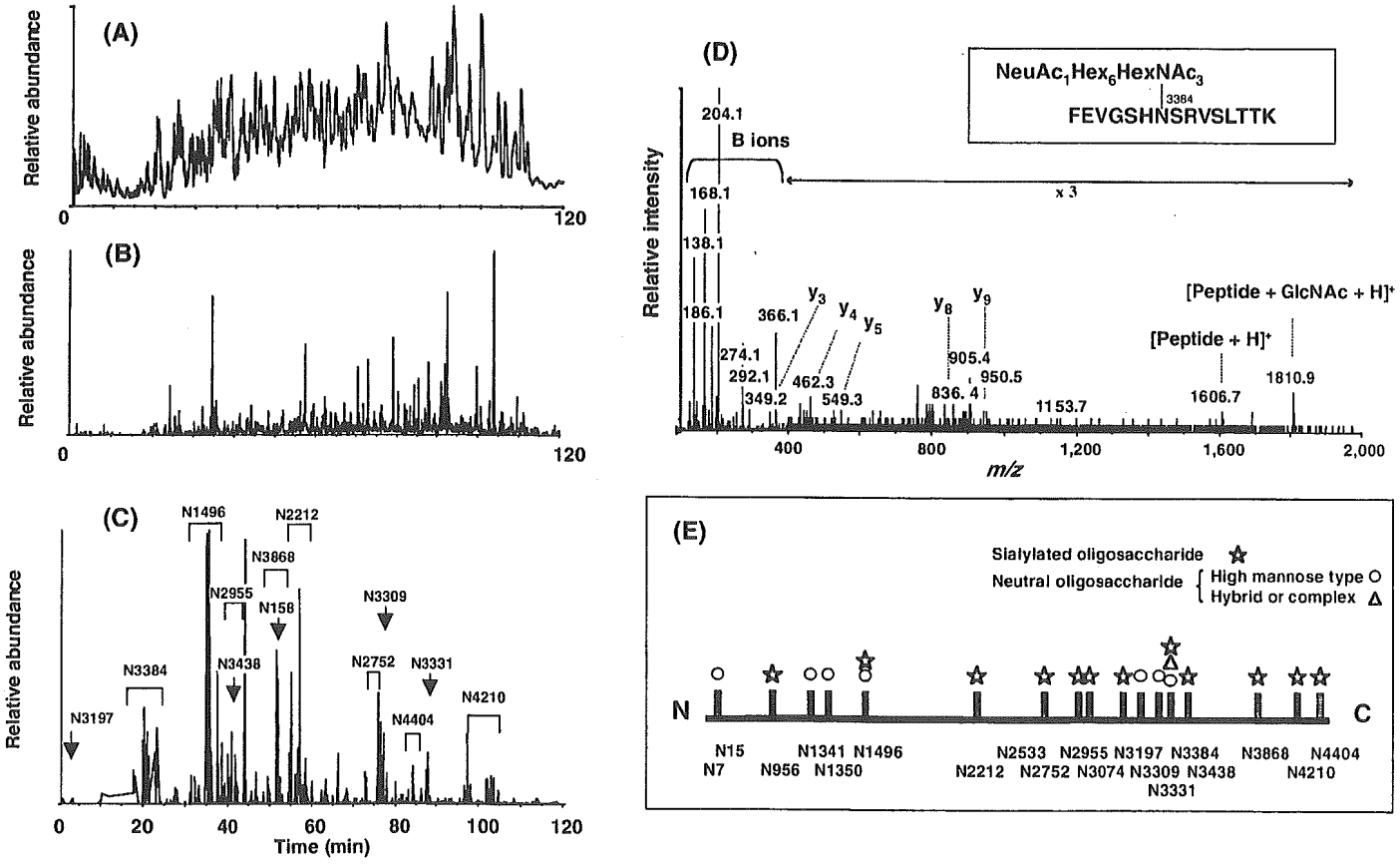

Fig. 8. Site-specific glycosylation analysis of apoB100 by LC/ESI-MS/MS. (A) TIC of full MS scan (*m/z* 400-2,000). (B) TIC of data-dependent CID-MS/MS scan (*m/z* 100-2,000). (C) Mass chromatogram at *m/z* 204 in data-dependent CID-MS/MS scan. (D) MS/MS spectrum of glycopeptide (precursor ion: *m/z* 1,160.4). (E) *N*-glycosylation of apoB100. Sample: tryptic digest of apoB100 (4 μg), LC: Paradigm (Michrome BioResources), Column: Magic C18 (0.2 × 50 mm, Michrome BioResources), MS: QSTAR (Applied Biosystems).

Here we demonstrate the site-specific glycosylation analysis of human apolipoprotein B100 (apoB100). Tryptic digest of apoB (4 μg) was injected into an LC/ESI-QqTOFMS instrument equipped with a C18 column. Figs. 8A and B are total ion chromatograms (TIC) obtained by full MS^1 scan and data-dependent CID-MS/MS scan, respectively (49). These chromatograms appear complicated due to a number of peptide-related ions derived from a large glycoprotein molecule of 500,000 Da. In order to localize glycopeptides in the peptide map, carbohydrate marker ion, $HexNAc^+$ at *m/z* 204, was extracted from the TIC of data-dependent CID-MS/MS scan (Fig. 8C). The MS/MS spectra of glycopeptides were then sorted from the peaks appearing in the mass chromatogram (Fig. 8D). We successfully identified 17 *N*-glycosylation sites among 19 potential *N*-glycosylation sites and deduced glycosylation at each glycosylation site from the mass of carbohydrate moieties (Fig. 8E).

F. Application in Proteomics and Glycomics

MS enables us to elucidate a small number of glycoproteins isolated by electrophoresis (67, 68) and micro HPLC (69). This method could be applied in comprehensive or carbohydrate structure-specific glycoprotein analysis by a combination with proteomic approaches such as 2-dimensional (2D) gel electrophoresis (GE) and 2D-LC followed by MS. Some applications have been already demonstrated, for instance, glycoprotein expression analysis using 2D-GE coupled with carbohydrate-specific dyeing or immunoblotting (70), and LC/MS combined with lectin affinity chromatography (71,72). These glycomic/proteomic technologies are expected to be a powerful tool for the functional study of glycoproteins, finding disease-related glycoproteins and identifying proteins attached to some glyco-epitopes.

プチドのMS/MSスペクトルを選び出す方法を見出した(49)。

図8に、我々が最近行ったオンライン法によるヒトアポリポプロテインB100 (apoB100)の部位特異的な糖鎖解析例を示す(49)。apoB100のトリプシン消化物(4 μg)をC18カラムを用いたLC/ESI-QqTOFMS装置で分析した。図8A及びBはフルMS^1スキャン(*m/z* 1,000-2,000)及びデータ依存的CID-MS/MSスキャンによって得られたトータルイオンクロマトグラム(TIC)である。apoB100は分子量約500,000 Daの大きな糖タンパク質なので、非常に多くのペプチドイオンが検出されている。そこで、糖ペプチドの溶出位置を推定するために、データ依存的CID-MS/MSスキャンによって生じた*m/z* 204イオンのみを抜き出した(図8C)。出現したピーク周辺からBイオンを指標に糖ペプチドのMS/MSスペクトルを探し出し、それらのスペクトル上のプロダクトイオンを帰属した(図8D)。その結果、19カ所の推定*N*結合型糖鎖結合部位のうち17カ所に糖鎖が結合していることを明らかにするとともに、それぞれの部位に結合している糖鎖を推定することができた(図8E)。

F. グライコミクス・プロテオミクスへの応用

現在では、電気泳動(67,68)やミクロ液体クロマトグラフィー(69)で分離された僅かな糖タンパク質からでも、MSによって、多くの糖鎖構造情報を得ることができるようになった。これらの糖鎖解析技術とプロテオミクス的アプローチ、すなわち、2次元電気泳動や2次元クロマトグラフィーによるタンパク質発現解析とMSを組み合わせることによって、糖タンパク質の網羅的解析や、任意の糖鎖構造を持つタンパク質の解析が可能になるものと期待されている。すでに、2次元電気泳動と糖タンパク質特異的染色法や免疫ブロットを組み合わせた糖タンパク質発現解析や(70)、レクチンアフィニティークロマトグラフィーと各種LC/MSを組み合わせた糖タンパク質の網羅的解析の例が報告されている(71,72)。今後、これらのグライコミクス・プロテオミクス解析技術が、糖鎖の機能研究や、疾患等に関与する糖鎖・糖タンパク質の探索、並びに様々な糖鎖エピトープ結合タンパク質の特定に貢献できるものと期待される。

References

1. Karas, M., and Hillenkamp, F. (1988) Anal. Chem. **60**, 2299–2301
2. Fenn, J. B., Mann, M., Meng, C. K., Wong, S. F., and Whitehouse, C. M. (1989) Science **246**, 64–71
3. Lemoine, J., Chirat, F., and Domon, B. (1996) J. Mass Spectrom. **31**, 908–912
4. Bahr, U., Pfenninger, A., Karas, M., and Stahl, B. (1997) Anal. Chem. **69**, 4530–4535
5. Hunt, D. F., Yates, J. R., 3rd, Shabanowitz, J., Winston, S., and Hauer, C. R. (1986) Proc. Natl. Acad. Sci. U S A. **83**, 6233–6237
6. Weiskopf, A. S., Vouros, P., and Harvey, D. J. (1998) Anal. Chem. **70**, 4441–4447
7. Naven, T. J., Harvey, D. J., Brown, J., and Critchley, G. (1997) Rapid Commun. Mass Spectrom. **11**, 1681–1686
8. Solouki, T., Reinhold, B. B., Costello, C. E., O'Malley, M., Guan, S., and Marshall, A. G. (1998) Anal. Chem. **70**, 857–864
9. Chai, W., Piskarev, V., and Lawson, A. M. (2001) Anal. Chem. **73**, 651–657
10. Harvey, D. J., Bateman, R. H., Bordoli, R. S., and Tyldesley, R. (2000) Rapid Commun. Mass Spectrom. **14**, 2135–2142
11. Sagi, D., Peter-Katalinic, J., Conradt, H. S., and Nimtz, M. (2002) J. Am. Soc. Mass Spectrom. **13**, 1138–1148
12. Zhang, S., and Chelius, D. (2004) J. Biomol. Tech. **15**, 120–133
13. Karlsson, N. G., Schulz, B. L., and Packer, N. H. (2004) J. Am. Soc. Mass Spectrom. **15**, 659–672
14. Domon, B., and Costello, C. E. (1988) Glycoconj. J. **5**, 397–409
15. Meisen, I., Peter-Katalinic, J., and Muthing, J. (2003) Anal. Chem. **75**, 5719–5725
16. Xue, J., Song, L., Khaja, S. D., Locke, R. D., West, C. M., Laine, R. A., and Matta, K. L. (2004) Rapid Commun. Mass Spectrom. **18**, 1947–1955

17. Takegawa, Y., Deguchi, K., Ito, S., Yoshioka, S., Sano, A., Yoshinari, K., Kobayashi, K., Nakagawa, H., Monde, K., and Nishimura, S. (2004) Anal Chem. **76**, 7294–7303
18. Takegawa, Y., Deguchi, K., Ito, S., Yoshioka, S., Nakagawa, H., and Nishimura, S. (2005) Rapid Commun. Mass Spectrom. **19**, 937–946
19. Harvey, D. J. (1999) Mass Spectrom. Rev. **18**, 349–450
20. Harvey, D. J., Bateman, R. H., and Green, M. R. (1997) J. Mass Spectrom. **32**, 167–187
21. Kawasaki, N., Ohta, M., Hyuga, S., Hashimoto, O., and Hayakawa, T. (1999) Anal. Biochem. **269**, 297–303
22. Kawasaki, N., Haishima, Y., Ohta, M., Itoh, S., Hyuga, M., Hyuga, S., and Hayakawa, T. (2001) Glycobiology **11**, 1043–1049
23. Sato, Y., Suzuki, M., Nirasawa, T., Suzuki, A., and Endo, T. (2000) Anal. Chem. **72**, 1207–1216
24. Takegawa, Y., Deguchi, K., Ito, S., Yoshioka, S., Nakagawa, H., and Nishimura, S. (2005) Anal. Chem. **77**, 2097–2106
25. Royle, L., Mattu, T. S., Hart, E., Langridge, J. I., Merry, A. H., Murphy, N., Harvey, D. J., Dwek, R. A., and Rudd, P. M. (2002) Anal. Biochem. **304**, 70–90
26. Hase, S., Ikenaka, T., and Matsushima, Y. (1981) J. Biochem. (Tokyo). **90**, 407–414
27. Suzuki-Sawada, J., Umeda, Y., Kondo, A., and Kato, I. (1992) Anal. Biochem. **207**, 203–207
28. Bigge, J. C., Patel, T. P., Bruce, J. A., Goulding, P. N., Charles, S. M., and Parekh, R. B. (1995) Anal. Biochem. **230**, 229–238
29. Ohta, M., Hamako, J., Yamamoto, S., Hatta, H., Kim, M., Yamamoto, T., Oka, S., Mizuochi, T., and Matsuura, F. (1991) Glycoconj. J. **8**, 400–413
30. Yoshimi, Y., Yamazaki, S., and Ikekita, M. (1999) Biochem. Biophys. Acta. **1426**, 69–79
31. Suzuki, S., Kakehi, K., and Honda, S. (1996) Anal. Chem. **68**, 2073–2083
32. Okamoto, M., Takahashi, K., and Doi, T. (1995) Rapid Commun. Mass Spectrom. **9**, 641–643
33. Lattova, E., and Perreault, H. (2003) J. Chromatogr. A. **1016**, 71–87
34. Morelle, W., Faid, V., and Michalski, J. C. (2004) Rapid Commun. Mass Spectrom. **18**, 2451–2464
35. Yoshino, K., Takao, T., Murata, H., and Shimonishi, Y. (1995) Anal. Chem. **67**, 4028–4031
36. Kawasaki, N., Ohta, M., Itoh, S., Hyuga, M., Hyuga, S., and Hayakawa, T. (2002) Biologicals. **30**, 113–123
37. Karlsson, N. G., Wilson, N. L., Wirth, H. J., Dawes, P., Joshi, H., and Packer, N. H. (2004) Rapid Commun. Mass Spectrom. **18**, 2282–2292
38. Zamfir, A., Seidler, D. G., Schonherr, E., Kresse, H., and Peter-Katalinic, J. (2004) Electrophoresis **25**, 2010–2016
39. Kremmer, T., Szollosi, E., Boldizsar, M., Vincze, B., Ludanyi, K., Imre, T., Schlosser, G., and Vekey, K. (2004) Biomed. Chromatogr. **18**, 323–329
40. Hashii, N., Kawasaki, N., Itoh, S., Hyuga, M., Kawanishi, T., and Hayakawa, T. (2005) Proteomics (in press)
41. Yuan, J., Hashii, N., Kawasaki, N., Itoh, S., Kawanishi, T., and Hayakawa, T. (2005) J. Chromatogr. A. **1067**, 145–152
42. Demelbauer, U. M., Zehl, M., Plematl, A., Allmaier, G., and Rizzi, A. (2004) Rapid Commun. Mass Spectrom. **18**, 1575–1582
43. Roepstorff, P., and Fohlman, J. (1984) Biomed. Mass Spectrom. **11**, 601
44. Hakansson, K., Chalmers, M. J., Quinn, J. P., McFarland, M. A., Hendrickson, C. L., and Marshall, A. G. (2003) Anal. Chem. **75**, 3256–3262
45. Hakansson, K., Cooper, H. J., Emmett, M. R., Costello, C. E., Marshall, A. G., and Nilsson, C. L. (2001) Anal. Chem. **73**, 4530–4536
46. Kurogochi, M., and Nishimura, S. (2004) Anal. Chem. **76**, 6097–6101
47. Krokhin, O., Ens, W., Standing, K. G., Wilkins, J., and Perreault, H. (2004) Rapid Commun. Mass Spectrom. **18**, 2020–2030
48. Wuhrer, M., Hokke, C. H., and Deelder, A. M. (2004) Rapid Commun. Mass Spectrom. **18**, 1741–1748
49. Harazono, A., Kawasaki, N., Kawanishi, T., and Hayakawa, T. (2005) Glycobiology **15**, 447–462
50. Nemeth, J. F., Hochgesang, G. P., Jr., Marnett, L. J., and Caprioli, R. M. (2001) Biochemistry **40**, 3109–3116
51. Hui, J. P., White, T. C., and Thibault, P. (2002) Glycobiology **12**, 837–849
52. Sandra, K., Devreese, B., Van Beeumen, J., Stals, I., and Claeyssens, M. (2004) J. Am. Soc. Mass Spectrom. **15**, 413–423
53. Sandra, K., Stals, I., Sandra, P., Claeyssens, M., Van Beeumen, J., and Devreese, B. (2004) J. Chromatogr. A. **1058**, 263–272
54. Satomi, Y., Shimonishi, Y., and Takao, T. (2004) FEBS Lett. **576**, 51–56
55. Wada, Y., Tajiri, M., and Yoshida, S. (2004) Anal. Chem. **76**, 6560–6565
56. Itoh, S., Kawasaki, N., Hashii, N., Harazono, A., Matsuishi, Y., Kawanishi, T., and Hayakawa, T. (2005) J. Chromatogr. A. Submitted
57. Garcia, R., Rodriguez, R., Montesino, R., Besada, V., Gonzalez, J., and Cremata, J. A. (1995) Anal. Biochem. **231**, 342–348
58. Fu, D., and van Halbeek, H. (1992) Anal. Biochem. **206**, 53–63
59. Carr, S. A., Huddleston, M. J., and Bean, M. F. (1993) Protein Sci. **2**, 183–196
60. Ethier, M., Saba, J. A., Spearman, M., Krokhin, O., Butler, M., Ens, W., Standing, K. G., and Perreault, H. (2003) Rapid Commun. Mass Spectrom. **17**, 2713–2720
61. Huddleston, M. J., Bean, M. F., and Carr, S. A. (1993) Anal. Chem. **65**, 877–884
62. Kapron, J. T., Hilliard, G. M., Lakins, J. N., Tenniswood, M. P., West, K. A., Carr, S. A., and Crabb, J. W. (1997) Protein Sci. **6**, 2120–2133
63. Medzihradszky, K. F., Besman, M. J., and Burlingame, A. L. (1997) Anal. Chem. **69**, 3986–3994
64. Ritchie, M. A., Gill, A. C., Deery, M. J., and Lilley, K. (2002) J. Am. Soc. Mass Spectrom. **13**, 1065–1077
65. Schindler, P. A., Settineri, C. A., Collet, X., Fielding, C. J., and Burlingame, A. L. (1995) Protein Sci. **4**, 791–803
66. Wang, F., Nakouzi, A., Angeletti, R. H., and Casadevall, A. (2003) Anal. Biochem. **314**, 266–280
67. Wilson, N. L., Schulz, B. L., Karlsson, N. G., and Packer, N. H. (2002) J. Proteome Res. **1**, 521–529
68. Itoh, S., Harazono, A., Kawasaki, N., Hashii, N., Matsuishi, Y., Kawanishi, T., and Hayakawa, T. (2004) J. Electrophoresis **48**, 163–168
69. Fan, X., She, Y. M., Bagshaw, R. D., Callahan, J. W., Schachter, H., and Mahuran, D. J. (2004) Anal. Biochem. **332**, 178–186
70. Higai, K., Shibukawa, K., Muto, S., and Matsumoto, K. (2003) Anal. Sci. **19**, 85–92
71. Kaji, H., Saito, H., Yamauchi, Y., Shinkawa, T., Taoka, M., Hirabayashi, J., Kasai, K., Takahashi, N., and Isobe, T. (2003) Nat. Biotechnol. **21**, 667–672
72. Qiu, R., and Regnier, F. E. (2005) Anal. Chem. **77**, 2802–2809

Received on June 3, 2005, accepted on July 19, 2005

Glycobiology vol. 15 no. 5 pp. 447–462, 2005
doi:10.1093/glycob/cwi033
Advance Access publication on December 22, 2004

Site-specific glycosylation analysis of human apolipoprotein B100 using LC/ESI MS/MS

Akira Harazono[1], Nana Kawasaki, Toru Kawanishi, and Takao Hayakawa

National Institute of Health Sciences, Division of Biological Chemistry and Biologicals, 1-18-1 Kami-yoga, Setagaya-Ku, Tokyo 158-8501, Japan

Received on 28 June 2004; revised on 24 November 2004; accepted on 16 December, 2004

Human apolipoprotein B100 (apoB100) has 19 potential *N*-glycosylation sites, and 16 asparagine residues were reported to be occupied by high-mannose type, hybrid type, and monoantennary and biantennary complex type oligosaccharides. In the present study, a site-specific glycosylation analysis of apoB100 was carried out using reversed-phase high-performance liquid chromatography coupled with electrospray ionization tandem mass spectrometry (LC/ESI MS/MS). ApoB100 was reduced, carboxymethylated, and then digested by trypsin or chymotrypsin. The complex mixture of peptides and glycopeptides was subjected to LC/ESI MS/MS, where product ion spectra of the molecular ions were acquired data-dependently. The glycopeptide ions were extracted and confirmed by the presence of carbohydrate-specific fragment ions, such as *m/z* 204 (HexNAc) and 366 (HexHexNAc), in the product ion spectra. The peptide moiety of glycopeptide was determined by the presence of the b- and y-series ions derived from its amino acid sequence in the product ion spectrum, and the oligosaccharide moiety was deduced from the calculated molecular mass of the oligosaccharide. The heterogeneity of carbohydrate structures at 17 glycosylation sites was determined using this methodology. Our data showed that Asn2212, not previously identified as a site of glycosylation, could be glycosylated. It was also revealed that Asn158, 1341, 1350, 3309, and 3331 were occupied by high-mannose type oligosaccharides, and Asn 956, 1496, 2212, 2752, 2955, 3074, 3197, 3438, 3868, 4210, and 4404 were predominantly occupied by mono- or disialylated oligosaccharides. Asn3384, the nearest N-glycosylation site to the LDL-receptor binding site (amino acids 3359–3369), was occupied by a variety of oligosaccharides, including high-mannose, hybrid, and complex types. These results are useful for understanding the structure of LDL particles and oligosaccharide function in LDL–receptor ligand binding.

Key words: apolipoprotein B100/glycopeptide/liquid chromatography electrospray mass spectrometry/product ion spectrum/*N*-linked oligosaccharide

Introduction

Low-density lipoprotein (LDL) is the main cholesterol carrier in human plasma, and a high serum level of LDL is involved in the development of atherosclerosis. LDL is originally secreted as very low-density lipoprotein (VLDL). VLDL is converted to LDL and then removed from the circulation. Apolipoprotein B100 (apoB100) is the only protein component of LDL and is the ligand recognized by the LDL receptor. The amino acid sequence of human apoB100 has been deduced by analysis of the apoB100 cDNA sequence (Chen *et al.*, 1986; Knott *et al.*, 1986; Law *et al.*, 1986; Yang *et al.*, 1986). Mature apoB100 consists of 4536 amino acids, and its molecular weight has been calculated to be 513 kDa. ApoB100 has 19 potential *N*-glycosylation sites (Asn-X-Ser/Thr), of which 16 asparagine residues are found to be glycosylated (Yang *et al.*, 1989). The carbohydrate moieties were linked to asparagine residues at the following 16 positions: 158, 956, 1341, 1350, 1496, 2752, 2955, 3074, 3197, 3309, 3331, 3384, 3438, 3868, 4210, and 4404. The carbohydrate structures of the *N*-linked sugar chains of human apoB100 were reported to be high-mannose, hybrid, and mono- and disialylated complex type oligosaccharides (Garner *et al.*, 2001; Taniguchi *et al.*, 1979).

The role of carbohydrate moieties of apoB100 has been investigated by several laboratories. The *N*-linked oligosaccharides at the amino terminus of human apoB100 are important for the assembly and secretion of VLDL (Vukmirica *et al.*, 2002). Seven of the *N*-glycans are predicted to occur close to the LDL–receptor binding region of apoB100 and seem to have an important role (Yang *et al.*, 1986, 1989). The carbohydrate composition of apoB100, particularly sialylation, has been considered to contribute to the atherogenic properties of LDL. However, Shireman and Fisher (1979) reported that they do not appear to play a significant role in the binding of apoB100 to the LDL receptor. Furthermore, the distribution and diversity of human apoB100 oligosaccharides isolated from normolipidemic, hypercholesterolemic, and hypertriglyceridemic diabetic subjects were highly conserved even when characterized in LDL subfractions (Garner *et al.*, 2001). The potential function of apoB100 carbohydrates posthepatic secretion is not well understood. Glycoproteins have a variety of sugar chains at each glycosylation site. Because of the individual functions at each site, a comparison of glycosylation among various sites is important. Therefore, to investigate the role of carbohydrate moieties of apoB100, we attempted to determine the carbohydrate heterogeneity site-specifically.

To determine the site-specific carbohydrate heterogeneity of glycoproteins, the glycoprotein must be digested into

[1]To whom correspondence should be addressed; e-mail: harazono@nihs.go.jp

peptides and glycopeptides, and then both the peptide and sugar chain of each glycopeptide must be analyzed. One of the most effective techniques for mapping proteolytic fragments of glycoproteins is liquid chromatography (LC) coupled with electrospray ionization (ESI) mass spectrometry (MS) (Carr *et al.*, 1993; Duffin *et al.*, 1992; Kawasaki *et al.*, 2004; Ling *et al.*, 1991). The specific detection of glycopeptides can be achieved by monitoring specific diagnostic sugar oxonium ions, such as *m/z* 204 (HexNAc) and 366 (HexHexNAc) produced by cone voltage fragmentation, or by precursor ion scanning (Carr *et al.*, 1993; Duffin *et al.*, 1992). However, when many *N*-glycosylation sites are present within a glycoprotein, the chromatogram becomes extremely complex and assignment of the glycopeptide ions is very difficult.

We present here an alternative strategy for the site-specific glycosylation analysis of a peptide and glycopeptide mixture using LC/ESI MS/MS, where we acquired the product ion spectrum for all significant molecular ions in a data-dependent manner. Product ion spectra of molecular ions allow the specific detection of glycopeptides from a complex mixture of peptides based on the presence of diagnostic sugar oxonium ions of oligosaccharides. Furthermore, this method allows confirmation of the amino acid sequence of a glycopeptide by the presence of b- and y-series fragment ions of the peptide. Using this method, we identified one previously unidentified *N*-glycosylated site of ApoB100 and determined the oligosaccharide heterogeneity of each of 17 *N*-glycosylation sites. Our findings provide information on the structure of apoB100 that will be useful to future studies on the structure, function, and metabolism of plasma LDL.

Results

Enzyme digestion

To determine the oligosaccharide heterogeneity at each glycosylation site, reduced and carboxymethylated apoB100 was digested into peptides and glycopeptides. Table I shows the amino acid sequences of the tryptic or chymotryptic peptides, including the putative *N*-glycosylation sites. The putative glycosylation sites were numbered (G1–19). Boldface indicates the previously reported *N*-glycosylation sites (G2–6 and G9–19). When apoB100 is digested by trypsin, potential *N*-glycosylation sites, Asn1341 (G4) and Asn1350 (G5), belong to the same peptide. Because chymotrypsin

Table I. The amino acid sequences of the tryptic or chymotryptic peptides including the putative *N*-glycosylation sites in apoB100

N-glycosylation site[a]		Tryptic digests		Chymotryptic digests	
Residue	ID	Sequence	Theoretical mass[b]	Sequence	Theoretical mass[b]
Asn^{7}	G1	EEEMLEN^{7}VSLVCPK	1677.8	EN^{7}VSL	560.3
Asn^{158}	**G2**	QVLFLDTVYGN^{158}CSTHFTVK	2229.1	GN^{158}CSTHF	822.3
Asn^{956}	**G3**	QVFPGLNYCTSGAYSN^{956}ASSTDSASYYPLTGDTR	3550.5	SN^{956}ASSTDSASY	1088.4
Asn^{1341}	**G4**	LYQLQVPLLGVLDLSTNVYSNLYN^{1341}	4692.3	N^{1341}W	318.1
Asn^{1350}	**G5**	WSASYSGGN^{1350}TSTDHFSLR		SGGN^{1350}TSTDHF	1021.4
Asn^{1496}	**G6**	FN^{1496}SSYLQGTNQITGR	1684.8	N^{1496}SSY	469.2
Asn^{2212}	G7	TIHDLHLFIENIDFN^{2212}K	1968.0	N^{2212}KSGSSTASW	1023.5
Asn^{2533}	G8	N^{2533}LTDFAEQYSIQDWAK	1928.9	AAKN^{2533}L	515.3
Asn^{2752}	**G9**	IQSPLFTLDANADIGN^{2752}GTTSANEAGIAASITAK	3231.6	DANADIGN^{2752} GTTSANEAGIAASITAKGESKL	2846.4
Asn^{2955}	**G10**	VNQNLVYESGSLN^{2955}FSK	1797.9	N^{2955}F	279.1
Asn^{3074}	**G11**	YNQN^{3074}FSAGNNENIMEAHVGINGEANLD FLNIPLTIPEMR	4359.1	NQN^{3074}F	521.2
Asn^{3197}	**G12**	SYN^{3197}ETK	740.3	N^{3197}ETKIKF	878.5
Asn^{3309}	**G13**	ELCTISHIFIPAMGN^{3309}ITYDFSFK	2704.3	IPAMGN^{3309}ITY	978.5
Asn^{3331}	**G14**	SSVITLNTNAELFN^{3331}QSDIVAHLLSSSSSVIDALQYK	3864.0	N^{3331}QSDIVAHL	995.5
Asn^{3384}	**G15**	FVEGSHN^{3384}STVSLTTK	1605.8	VEGSHN^{3384}STVSL	1128.5
Asn^{3438}	**G16**	YDFN^{3438}SSMLYSTAK	1525.7	N^{3438}SSML	550.2
Asn^{3868}	**G17**	FEVDSPVYN^{3868}ATWSASLK	1912.9	N^{3868}ATW	490.2
Asn^{4210}	**G18**	VHN^{4210}GSEILFSYFQDLVITLPFELR	2836.5	SKVHN^{4210}GSEIL	1082.6
Asn^{4404}	**G19**	DFHSEYIVSASN^{4404}FTSQLSSQVEQFLHR	3155.5	IVSASN^{4404}F	736.4

Human apoB100 amino acid sequence (NP_000375. apolipoprotein B [gi:4502153]) was obtained from the NCBI database (www.ncbi.nlm.nih.gov/pubmed). Boldface indicates previously reported *N*-glycosylation sites. Cystein residue was carboxymethylated, and carboxymethylated cystein was underscored.

[a]Potential *N*-glycosylation sites were identified with the consensus sequence NXS/T, where X is any amino acid except P.

[b]Monoisotopic mass value.

can cleave apoB100 into glycopeptides containing one glycosylation site, we attempted to analyze both proteolytic fragments from trypsin digestion and chymotrypsin digestion to identify the site-specific glycosylation.

LC/ESI MS/MS analysis of tryptic digest of apoB100

The schema of a site-specific glycosylation analysis of apoB100 is shown in Figure 1. A mixture of peptides and glycopeptides was subjected to LC/ESI MS/MS with a reversed-phase column. Figure 2A shows a total ion chromatogram (TIC) of a time-of-flight (TOF) MS scan for the full scan *m/z* 1000–2000. When double or higher charged molecular ions were detected, the product ion spectrum was automatically acquired. Figure 2B shows a TIC of the product ion scan. The collision energy at the second quadrupole for the product ion scan was adjusted from 50 to 80 eV depending on the size and charge of the precursor ion. Under these conditions, peptide precursor ions produced b- and y-series fragment ions derived from its amino acid sequence (data not shown), and glycopeptide precursor ions produced abundant carbohydrate-specific ions, *m/z* 204, 186, 168, and 366 (described later). The intensity of ions at *m/z* 204.05–204.15 (HexNAc, 204.08) in each product ion scan are illustrated in Figure 2C. The extracted ion chromatogram at *m/z* 204 (Figure 2C) and 366 (data not shown) provides useful information on the selection of glycopeptide precursor ions. The product ion spectra of glycopeptides show a very characteristic pattern (see later figures). There were intense oligosaccharide-derived peaks of *m/z* 204 (HexNAc), 366 (HexHexNAc), 186 (HexNAc–H_2O), and 168 (HexNAc–$2H_2O$), and if present, 163 (Hex), 292 (Neu5Ac), and 274 (Neu5Ac–H_2O). Therefore, we can very easily distinguish the glycopeptide precursor ions from peptide ions. As expected, many parent ions having 204 and

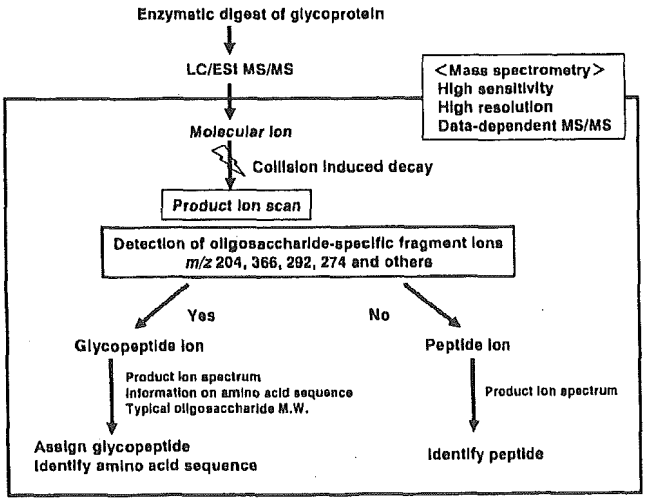

Fig. 1. Schema of site-specific glycosylation analysis. Glycoprotein was digested into peptides and glycopeptides containing only one glycosylation site. Only LC/ESI MS/MS was used. Data-dependent MS/MS acquisition was used to differentiate glycopeptide ions from peptide ions and identify the amino acid sequence of the glycopeptides. The oligosaccharide structure was deduced based on the calculated oligosaccharide molecular weight.

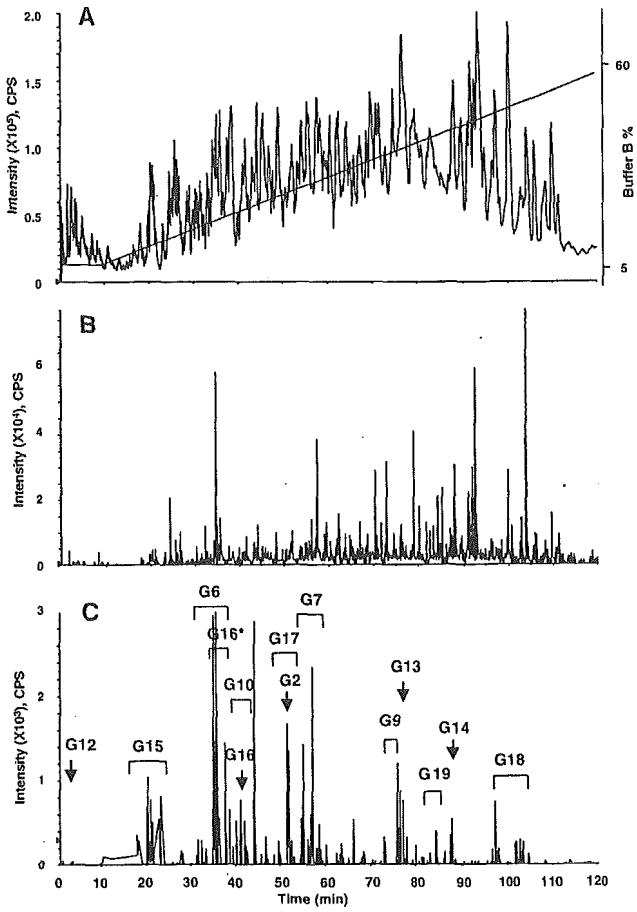

Fig. 2. LC/ESI MS/MS of tryptic digest of apolipoprotein B100. TIC of the TOF MS scan for the full scan *m/z* 1000–2000 and the HPLC gradient are indicated (**A**). TIC of the product ion scan data-dependently acquired (**B**). Extract ion chromatogram at *m/z* 204 of product ion spectra (**C**). Arrows and brackets denote glycopeptide fraction and *N*-glycosylation site ID. G16* was found to be oxidized at a methionine residue.

366 fragment ions in the product ion spectrum were detected, and most of these precursor ions were found as glycopeptides.

The glycopeptides were assigned based on an examination of product ion spectra using the information on the peptides containing a putative *N*-glycosylation site. Figures 3A, 3B, and 3C show the product ion spectra of 1412.1 (+2) at 18 min, 1160.4 (+3) at 20 min and 1271.1 (+3) at 22 min for the glycopeptides. There were intense carbohydrate B^+ ions such as *m/z* 204 (HexNAc), 366 (HexHexNAc), and 186 (HexNAc–H_2O) and other weak peaks in the product ion spectra. These product ion spectra were very similar to each other (Figure 3A, 3B, and 3C). Careful examination of these product ion spectra for the glycopeptides revealed that several fragment ions were consistent with b- and y-series fragment ions derived from the peptide FVEGSHNSTVS-LTTK (residue 3378–3392). The deduced b- and y-series fragment ions of the peptide FVEGSHNSTVSLTTK were listed, and the fragment ions detected in the product ion spectrum of 1160.4 (+3) are underscored in the table (Figure 3D). The molecular ions of the peptide (*m/z* 1606) and

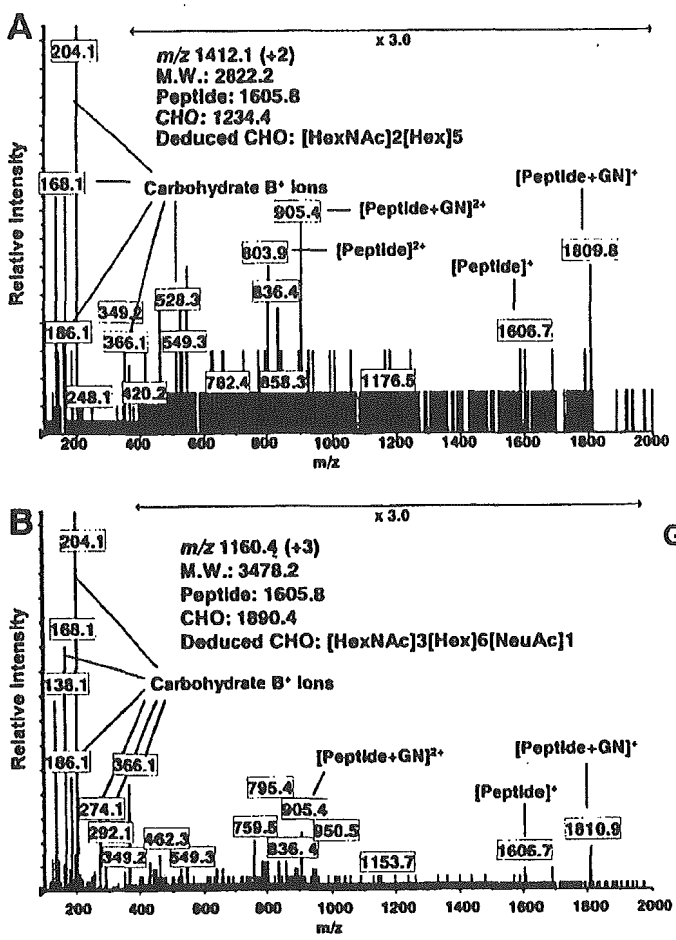

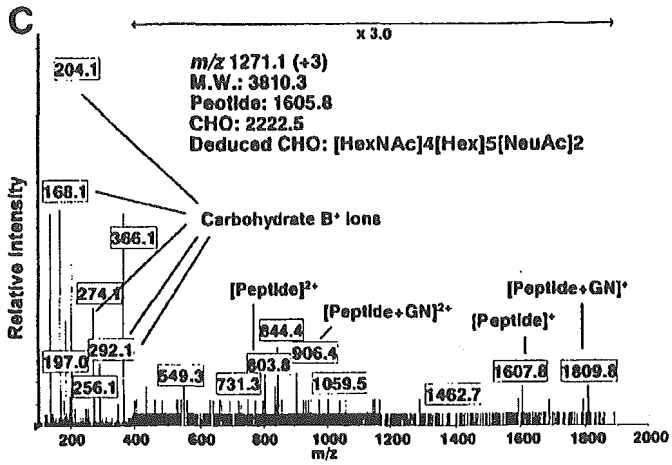

D

G15

Residue	Mass	b	b-NH3	y	y-NH3
F	147.1	148.1	131.0	1606.8	1589.8
V	99.1	247.1	230.1	1459.7	1442.7
E	129.0	376.2	359.1	1360.7	1343.6
G	57.0	433.2	416.2	1231.7	1214.6
S	87.0	520.2	503.2	1174.6	1157.6
H	137.1	657.3	640.3	1087.6	1070.5
(N)	114.0	771.3	754.3	950.5	933.5
S	87.0	858.4	841.3	836.5	819.4
T	101.0	959.4	942.4	749.4	732.4
V	99.1	1058.5	1041.5	648.4	631.4
S	87.0	1145.5	1128.5	549.3	532.3
L	113.1	1258.6	1241.6	462.3	445.3
T	101.0	1359.7	1342.6	349.2	332.2
T	101.0	1460.7	1443.7	248.2	231.1
K	128.1	1588.8	1571.8	147.1	130.1

Fig. 3. Product ion spectra of the *N*-glycosylated peptides containing Asn3384 (G15). Product ion scan of *m/z* 1412.1 (+2) (**A**), 1160.4 (+3) (**B**), and 1271.1 (+3) (**C**) at 18, 20, and 22 min, respectively. These spectra show a characteristic fragmentation pattern with abundant carbohydrate-diagnostic oxonium ions at 163, 168, 186, 204, and 366 and very similar patterns to each other. The oxonium ions at m/z 292 (Neu5Ac) and 274 (Neu5A-H2O) were observed in the peptides having sialylated oligosaccharide (**B**) and (**C**). Several fragment ions are consistent with the b- and y-series fragment ions derived from the peptide FVEGSHNSTVSLTTK (residue 3378–3392). $[Peptide]^+$ and $[peptide+GlcNAc]^+$ ions were also detected. (**D**) shows *m/z* of the proposed b- and y-series fragment ions of the peptide and the fragment ions detected in Figure 3B are underscored. Based on the calculated oligosaccharide mass, the deduced oligosaccharide structure was presented. GN, *N*-acetylglucosamine.

peptide + GlcNAc (*m/z* 1809) were also detected in the product ion spectra (Figure 3A, 3B, and 3C). These results suggest that these glycopeptides have the same peptide, FVEGSHNSTVSLTTK, including the *N*-glycosylation site Asn3384 (G15). Carbohydrate molecular weight was calculated by subtracting the theoretical molecular weight of the peptide (1605.8) from the calculated molecular weight of the glycopeptide and adding the molecular weight of H_2O (18.0). The oligosaccharide structure was deduced based on the molecular weight and previously reported oligosaccharides of apoB100. The presence of product ions at *m/z* 274 (Neu5Ac–H_2O) and 292 (Neu5Ac) suggested that those at *m/z* 1160.4 (+3) and 1271.1 (+3) were glycopeptide ions having sialylated oligosaccharides. Thus the carbohydrate compositions, $[HexNAc]_2[Hex]_5$, $[HexNAc]_3[Hex]_6[Neu5Ac]_1$, and $[HexNAc]_4[Hex]_5[Neu5Ac]_2$, were deduced from the carbohydrate molecular weights, 1234.4, 1890.4, and 2222.5, respectively.

Figures 4 shows the product ion spectra of 1294.8 (+3) at 55 min and 1152.7 (+3) at 35 min for other glycopeptides. There are intense carbohydrate B^+ ions in the product ion spectra. Several ions consisting of b- and y-series fragment ions from the peptide TIHDLHLFIENIDHNK (residue 2198–2213) were found in the product ion spectrum of 1294.8 (+3) (Figure 4A), and detected ions are underscored in the table. The molecular ions of the peptide (*m/z* 1968.9) were also detected in the product ion spectra. The carbohydrate molecular weight was calculated from the molecular weight of the peptide, 1968.0, and the molecular weight of the glycopeptide, 3881.4. Carbohydrate composition was deduced from the carbohydrate molecular weight (1931.4) and presence of Neu5Ac. Thus, the peptide moiety TIHDLHLFIENIDHNK and carbohydrate composition $[HexNAc]_4[Hex]_5[Neu5Ac]_1$ were suggested.

Many ions in the product ion spectrum of 1152.7 (+3) were consistent with the b- and y-series fragment ions

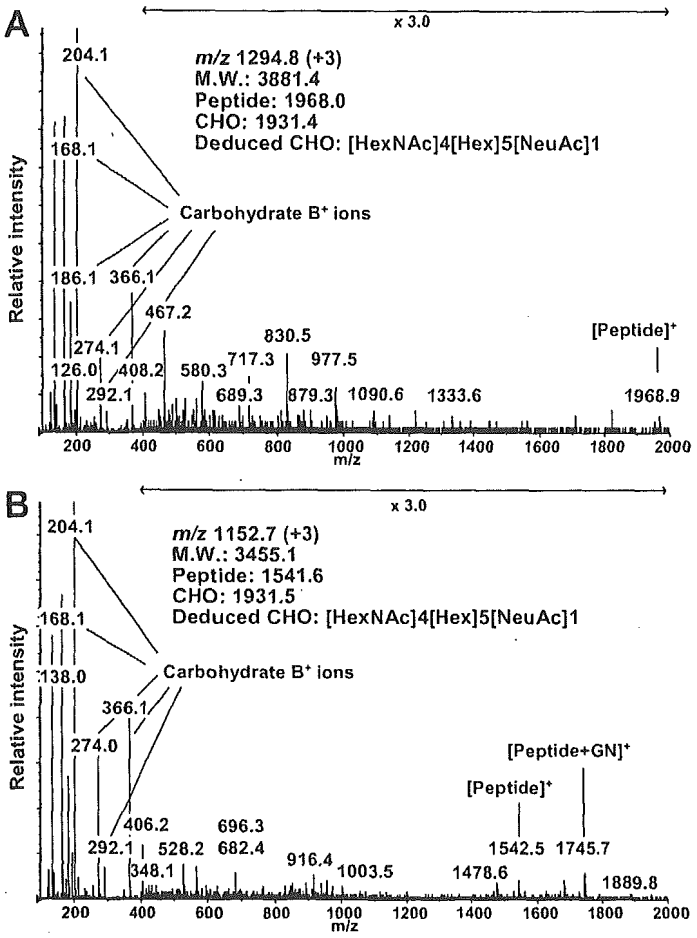

G7

Residue	Mass	b	b-NH3	y	y-NH3
T	101.0	102.1	85.0	1969.0	1952.0
I	113.1	215.1	198.1	1868.0	1850.9
H	137.1	352.2	335.2	1754.9	1737.9
D	115.0	467.2	450.2	1617.8	1600.8
L	113.1	580.3	563.3	1502.8	1485.8
H	137.1	717.4	700.3	1389.7	1372.7
L	113.1	830.5	813.4	1252.7	1235.6
F	147.1	977.5	960.5	1139.6	1122.5
I	113.1	1090.6	1073.6	992.5	975.5
E	129.0	1219.6	1202.6	879.4	862.4
N	114.0	1333.7	1316.7	750.4	733.4
I	113.1	1446.8	1429.7	636.3	619.3
D	115.0	1561.8	1544.8	523.3	506.2
F	147.1	1708.9	1691.8	408.2	391.2
(N)	114.0	1822.9	1805.9	261.2	244.1
K	128.1	1951.0	1934.0	147.1	130.1

G16

Residue	Mass	b	b-NH3	y	y-NH3
Y	163.1	164.1	147.0	1542.7	1525.7
D	115.0	279.1	262.1	1379.6	1362.6
F	147.1	426.2	409.1	1264.6	1247.6
(N)	114.0	540.2	523.2	1117.5	1100.5
S	87.0	627.2	610.2	1003.5	986.5
S	87.0	714.3	697.2	916.4	899.4
M(O)	147.0	861.3	844.3	845.4	828.4
L	113.1	974.4	957.4	682.4	665.4
Y	163.1	1137.5	1120.4	569.3	552.3
S	87.0	1224.5	1207.5	406.2	389.2
T	101.0	1325.5	1308.5	319.2	302.2
A	71.0	1396.6	1379.6	218.1	201.1
K	128.1	1524.7	1507.6	147.1	130.1

Fig. 4. Product ion spectra of the tryptic *N*-glycosylated peptides of apoB100. (**A**) Product ion spectrum of *m/z* 1294.8 (+3) at 55 min for the glycopeptide containing Asn2212 (G7). Several ions are consistent with the b- and y-series fragment ions derived from the peptide TIHDLHLFIENIDFNK (residue 2198–2213). Table shows *m/z* of the proposed b- and y-series fragment ions and the detected ions are underscored. (**B**) Product ion spectrum of *m/z* 1152.7 (+3) at 35 min for the glycopeptide containing Asn3438 (G16) with oxidized methionine. The methionine residue at 3441 was considered oxidized. Several ions are consistent with the b- and y-series fragment ions derived from the peptide YDFNSSM(O)LYSTAK (residue 3435–3447). Table shows *m/z* of the proposed b- and y-series fragment ions and the detected ions are underscored. M(O), oxidized methionine.

derived from the peptide YSFNSSMLYSTAK (Figure 4B). However, the deduced peptide ion *m/z* at 1526.7 and peptide + GlcNAc at 1729.8 were not detected. The difference of 203 between the product ions at *m/z* 1542.5 and 1745.7 suggests that the molecular weight of the peptide moiety may be 1541.5, and an increase in mass of 16 Da suggests that the methionine residue of YSFNSSMLYSTAK (residue 3435–3447, molecular weight 1525.7) was oxidized. The deduced b- and y-series fragment ions of the peptide, YSFNSSMLYSTAK, with the oxidized methionine are listed and detected peptide fragment ions are underscored. Thus, the product ions at *m/z* 1542.5 and 1745.7 were considered the peptide and peptide + GlcNAc ions, respectively. Our method identified unexpected oxidization of methionine residue (Figure 4B). The carbohydrate molecular weight was calculated, and the carbohydrate composition, $[HexNAc]_4[Hex]_5[Neu5Ac]_1$, was deduced from the carbohydrate molecular weight, 1931.4, and presence of Neu5Ac.

Results of site-specific glycosylation analysis from tryptic digest are summarized in Table II. To avoid misassignment, only ions that were confirmed as glycopeptides by the product ion spectra or coeluting ions with glycopeptides were listed. We determined 13 of the 19 potential *N*-glycosylation sites and the oligosaccharide heterogeneity at each site in a site-specific glycosylation analysis of the tryptic digest of apoB100. The type of oligosaccharide was deduced based on the oligosaccharide composition. Glycopeptides containing *N*-glycosylation sites Asn7, 956, 1341, 1350, 2533, and 3074 (G1, 3, 4, 5, 8, and 11) could not be detected. The relative peak intensity does not accurately express the relative amount of glycoforms, because of the different ionization efficiency of each glycoform, different detection sensitivity at *m/z*, and simultaneous acquision of MS and MS/MS spectra. However, the relative peak intensity of each glycopeptide would provide an indication of the distribution in glycoforms.

Table II. Site-specific glycosylation analysis of the tryptic digest of apoB100 using LC/ESI MS/MS

			Glycopeptides			Oligosaccharide				
Glycosylation site ID	Retention time (min)	Peptide theoretical MW[a]	*m/z*	Charge	Calculated MW[a]	Calculated MW[a]	Theoretical MW[a]	Relative peak intensity (%)[b]	Composition[c]	Deduced Type[c]
G1	—	1677.8	—	—	—	—	—	—	—	—
G2	51	2229.1	1365.6	+3	4093.8	1882.7	1882.6	7	[HexNAc]2[Hex]9	High mannose
	51	2229.1	1311.6	+3	3931.7	1720.6	1720.6	13	[HexNAc]2[Hex]8	High mannose
	51	2229.1	1257.5	+3	3769.5	1558.4	1558.5	22	[HexNAc]2[Hex]7	High mannose
	51	2229.1	1203.5	+3	3607.6	1396.6	1396.5	13	[HexNAc]2[Hex]6	High mannose
	51	2229.1	1149.5	+3	3445.5	1234.4	1234.4	100	[HexNAc]2[Hex]5	High mannose
	51	2229.1	1723.7	+2	3445.4	1234.4				
G3	—	3550.5	—	—	—	—	—	—	—	—
G4, G5	—	4692.3	—	—	—	—	—	—	—	—
G6	33	1684.8	1451.6	+2	2901.2	1234.4	1234.4	15	[HexNAc]2[Hex]5	High mannose
	34	1684.8	1200.4	+3	3598.2	1931.4	1931.7	100	[HexNAc]4[Hex]5[Neu5Ac]1	Biantennary complex
	34	1684.8	1800.1	+2	3598.2	1931.4				
	35	1684.8	1146.4	+3	3436.2	1769.4	1769.6	23	[HexNAc]4[Hex]4[Neu5Ac]1	Biantennary complex
	35	1684.8	1719.2	+2	3436.4	1769.6				
	35	1684.8	1078.7	+3	3233.1	1566.3	1566.6	11	[HexNAc]3[Hex]4[Neu5Ac]1	Monoantennary complex
	35	1684.8	1132.8	+3	3395.4	1728.6	1728.6	5	[HexNAc]3[Hex]5[Neu5Ac]1	Hybrid
	35	1684.8	1186.8	+3	3557.4	1890.6	1890.7	3	[HexNAc]3[Hex]6[Neu5Ac]1	Hybrid
	35	1684.8	1240.8	+3	3719.4	2052.6	2052.7	3	[HexNAc]3[Hex]7[Neu5Ac]1	Hybrid
	37	1684.8	1297.4	+3	3889.2	2222.4	2222.8	24	[HexNAc]4[Hex]5[Neu5Ac]2	Biantennary complex
	37	1684.8	1945.7	+2	3889.4	2222.6				
G7	54	1968.0	1294.8	+3	3881.4	1931.4	1931.7	66	[HexNAc]4[Hex]5[Neu5Ac]1	Biantennary complex
	58	1968.0	1044.2	+4	4172.8	2222.8	2222.8	100	[HexNAc]4[Hex]5[Neu5Ac]2	Biantennary complex
	58	1968.0	1391.9	+3	4172.7	2222.7				
G8	—	1928.9	—	—	—	—	—	—	—	—
G9	73	3231.6	1360.4	+4	5437.6	2224.0	2222.8	—	[HexNAc]4[Hex]5[Neu5Ac]2	Biantennary complex
G10	40	1797.9	1238.1	+3	3711.3	1931.4	1931.7	41	[HexNAc]4[Hex]5[Neu5Ac]1	Biantennary complex
	41	1797.9	1856.7	+2	3711.4	1931.5				

Table II. continued

Glycosylation site ID	Retention time (min)	Peptide theoretical MW[a]	Glycopeptides *m/z*	Charge	Calculated MW[a]	Oligosaccharide Calculated MW[a]	Theoretical MW[a]	Relative peak intensity (%)[b]	Composition[c]	Deduced Type[c]
	43	1797.9	1001.6	+4	4002.4	2222.5	2222.8	100	[HexNAc]4[Hex]5[Neu5Ac]2	Biantennary complex
	43	1797.9	1335.1	+3	4002.3	2222.4				
G11	—	4359.1	—	—	—	—	—	—	—	—
G12	2	740.3	1473.6	+2	2945.2	2222.9	2222.8	—	[HexNAc]4[Hex]5[Neu5Ac]2	Biantennary complex
G13	75	2704.3	1102.7	+4	4406.8	1720.5	1720.6	22	[HexNAc]2[Hex]8	High mannose
	75	2704.3	1470.0	+3	4406.9	1720.6				
	76	2704.3	1062.2	+4	4244.8	1558.5	1558.5	54	[HexNAc]2[Hex]7	High mannose
	76	2704.3	1415.9	+3	4244.7	1558.4				
	76	2704.3	1021.6	+4	4082.4	1396.1	1396.5	100	[HexNAc]2[Hex]6	High mannose
	76	2704.3	1361.9	+3	4082.7	1396.4				
	76	2704.3	1307.9	+3	3920.7	1234.4	1234.4	50	[HexNAc]2[Hex]5	High mannose
G14	88	3864.0	1146.7	+5	5728.7	1882.7	1882.6	—	[HexNAc]2[Hex]9	High mannose
	88	3864.0	1433.1	+4	5728.3	1882.3				
G15	17	1605.8	1063.4	+3	3187.2	1599.4	1599.6	8	[HexNAc]3[Hex]6	Hybrid
	17	1605.8	1077.0	+3	3228.0	1640.2	1640.6	20	[HexNAc]4[Hex]5	Biantennary complex
	17	1605.8	1009.4	+3	3025.2	1437.4	1437.5	20	[HexNAc]3[Hex]5	Hybrid
	18	1605.8	1513.6	+2	3025.3	1437.5				
	18	1605.8	1023.0	+3	3066.0	1478.2	1478.5	13	[HexNAc]4[Hex]4	Biantennary complex
	18	1605.8	1412.1	+2	2822.2	1234.4	1234.4	4	[HexNAc]2[Hex]5	High mannose
	20	1605.8	1174.1	+3	3519.3	1931.5	1931.7	100	[HexNAc]4[Hex]5[Neu5Ac]1	Biantennary complex
	20	1605.8	1760.7	+2	3519.4	1931.6				
	20	1605.8	1160.4	+3	3478.2	1890.4	1890.7	10	[HexNAc]3[Hex]6[Neu5Ac]1	Hybrid
	20	1605.8	1106.4	+3	3316.2	1728.4	1728.6	94	[HexNAc]3[Hex]5[Neu5Ac]1	Hybrid
	20	1605.8	1659.2	+2	3316.4	1728.6				
	20	1605.8	1222.8	+3	3665.4	2077.6	2077.7	4	[HexNAc]4[Hex]5[Neu5Ac]1[Fuc]1	Biantennary complex
	20	1605.8	1052.4	+3	3154.2	1566.4	1566.6	42	[HexNAc]3[Hex]4[Neu5Ac]1	Monoantennary complex
	20	1605.8	1578.2	+2	3154.4	1566.6				
	21	1605.8	1120.0	+3	3357.0	1769.2	1769.6	23	[HexNAc]4[Hex]4[Neu5Ac]1	Biantennary complex
	22	1605.8	1271.1	+3	3810.3	2222.5	2222.8	49	[HexNAc]4[Hex]5[Neu5Ac]2	Biantennary complex
G16	42	1525.7	1147.4	+3	3439.2	1931.5	1931.7	—	[HexNAc]4[Hex]5[Neu5Ac]1	Biantennary complex
	42	1525.7	1720.7	+2	3439.3	1931.6				
	35	1541.7*	1152.7	+3	3455.1	1931.4	1931.7	100	[HexNAc]4[Hex]5[Neu5Ac]1	Biantennary complex

Table II. continued

Glycosylation site ID	Retention time (min)	Peptide theoretical MW[a]	Glycopeptides			Oligosaccharide			Composition[c]	Deduced Type[c]
			m/z	Charge	Calculated MW[a]	Calculated MW[a]	Theoretical MW[a]	Relative peak intensity (%)[b]		
	35	1541.7*	1728.6	+2	3455.2	1931.5				
	36	1541.7*	1098.7	+3	3293.1	1769.4	1769.6	9	[HexNAc]4[Hex]4[Neu5Ac]1	Biantennary complex
	36	1541.7*	1647.6	+2	3293.2	1769.5				
	36	1541.7*	1546.1	+2	3090.2	1566.5	1566.6	18	[HexNAc]3[Hex]4[Neu5Ac]1	Monoantennary complex
	38	1541.7*	1249.8	+3	3746.4	2222.7	2222.8	19	[HexNAc]4[Hex]5[Neu5Ac]2	Biantennary complex
G17	51	1912.9	1276.5	+3	3826.5	1931.6	1931.7	100	[HexNAc]4[Hex]5[Neu5Ac]1	Biantennary complex
	51	1912.9	1914.3	+2	3826.6	1931.7				
	54	1912.9	1495.3	+3	4482.9	2588.0	2587.9	6	[HexNAc]5[Hex]6[Neu5Ac]2	Triantennary complex
	54	1912.9	1030.4	+4	4117.6	2222.7	2222.8	39	[HexNAc]4[Hex]5[Neu5Ac]2	Biantennary complex
	54	1912.9	1373.5	+3	4117.5	2222.6				
G18	98	2836.5	1188.5	+4	4750.2	1931.7	1931.7	100	[HexNAc]4[Hex]5[Neu5Ac]1	Biantennary complex
	98	2836.5	1584.4	+3	4750.1	1931.7				
	98	2836.5	1148.0	+4	4588.1	1769.6	1769.6	10	[HexNAc]4[Hex]4[Neu5Ac]1	Biantennary complex
	102	2836.5	1009.3	+5	5041.3	2222.8	2222.8	64	[HexNAc]4[Hex]5[Neu5Ac]2	Biantennary complex
	102	2836.5	1261.6	+4	5042.2	2223.7				
	103	2836.5	1681.5	+3	5041.5	2223.0				
G19	83	3155.5	1014.8	+5	5069.0	1931.5	1931.7	79	[HexNAc]4[Hex]5[Neu5Ac]1	Biantennary complex
	86	3155.5	1073.1	+5	5360.5	2223.0	2222.8	100	[HexNAc]4[Hex]5[Neu5Ac]2	Biantennary complex

[a]Monoisotopic mass value.
[b]Relative peak intensity was calculated by comparing same charge state glycopeptide ions. The intensity of glycoform with maximum intensity at each glycosylation site was considered as 100%.
[c]The oligosaccharide composition and type were deduced from its composition.
*The glycopeptides including G16 were found to be oxidized at methionine residue.